AD-A063 618 PENNSYLVANIA STATE UNIV UNIVERSITY PARK APPLIED RESE--ETC F/G 17/1
DOPPLER SHIFT IN LAYERED MEDIA.(U)
AUG 78 R A KOLANO N00017-73-C-1418
UNCLASSIFIED TM-78-210 NL

| OF |
AD A063618

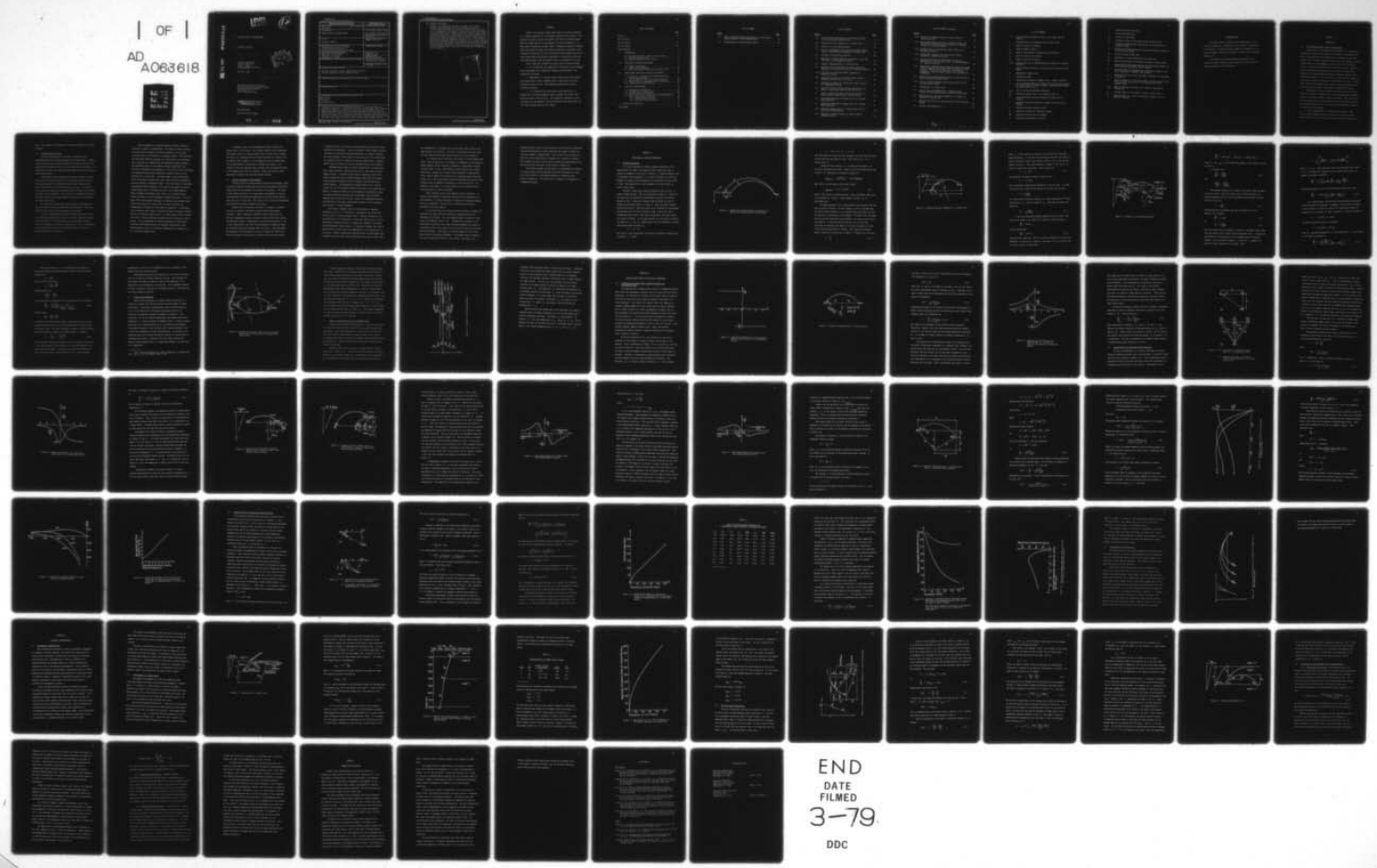

END
DATE FILMED
3-79
DDC

DOPPLER SHIFT IN LAYERED MEDIA

Richard A. Kolano

Technical Memorandum
File No. TM 78-210
August 3, 1978
Contract N00017-73-C-1418

Copy No. 15

Master's Thesis

80 p.

TM-78-210

The Pennsylvania State University
Institute for Science and Engineering
APPLIED RESEARCH LABORATORY
Post Office Box 30
State College, PA 16801

NAVY DEPARTMENT

NAVAL SEA SYSTEMS COMMAND

UNCLASSIFIED

SECURITY CLASSIFICATION OF THIS PAGE (When Data Entered)

REPORT DOCUMENTATION PAGE		READ INSTRUCTIONS BEFORE COMPLETING FORM
1. REPORT NUMBER TM 78-210	2. GOVT ACCESSION NO.	3. RECIPIENT'S CATALOG NUMBER
4. TITLE (and Subtitle) DOPPLER SHIFT IN LAYERED MEDIA		5. TYPE OF REPORT & PERIOD COVERED M.S. Thesis, November 1978
		6. PERFORMING ORG. REPORT NUMBER TM 78-210
7. AUTHOR(s) Richard A. Kolano		8. CONTRACT OR GRANT NUMBER(s) N00017-73-C-1418
9. PERFORMING ORGANIZATION NAME AND ADDRESS The Pennsylvania State University Applied Research Laboratory P. O. Box 30, State College, PA 16801		10. PROGRAM ELEMENT, PROJECT, TASK AREA & WORK UNIT NUMBERS
11. CONTROLLING OFFICE NAME AND ADDRESS Naval Sea Systems Command Department of the Navy Washington, DC 20362		12. REPORT DATE August 3, 1978
		13. NUMBER OF PAGES 88 pages & figures
14. MONITORING AGENCY NAME & ADDRESS(if different from Controlling Office)		15. SECURITY CLASS. (of this report) Unclassified, Unlimited
		15a. DECLASSIFICATION/DOWNGRADING SCHEDULE

16. DISTRIBUTION STATEMENT (of this Report)

Approved for public release, distribution unlimited,
per NSSC (Naval Sea Systems Command), 9/1/78

17. DISTRIBUTION STATEMENT (of the abstract entered in Block 20, if different from Report)

18. SUPPLEMENTARY NOTES

19. KEY WORDS (Continue on reverse side if necessary and identify by block number)

doppler shift
layered media
ray tracing
velocity gradients

20. ABSTRACT (Continue on reverse side if necessary and identify by block number)

Acoustic ray tracing in media where there are velocity gradients is a standard technique for a stationary transmitter and receiver. Also, dealing with moving sources and receivers and with the ensuing Doppler shifts is common practice in the absence of velocity gradients, i.e., when sound ray paths are straight lines. Although calculation of Doppler shifts when sound ray paths are curved are implicit in that part of the literature dealing with the total sound field, some interesting relations remain hidden when the

DD FORM 1 JAN 73 1473 EDITION OF 1 NOV 65 IS OBSOLETE

UNCLASSIFIED

SECURITY CLASSIFICATION OF THIS PAGE (When Data Entered)

20. ABSTRACT (Continued)

problem is considered in such general terms and only become apparent when the Doppler effect is considered on its own.

Such a study was conducted, its major results being as follows: 1) It is shown that the range rate of the source can be estimated from a knowledge of the transmitted frequency and the angle of the reception of the sound. 2) When there is a vertical offset between source and receiver, the Doppler shift reaches a maximum value at some finite horizontal separation between the two. The equations governing the specific relations are given. 3) It is shown how the error may be calculated when it is assumed that the sound propagates along a straight line rather than along the actual curved ray path. The significant parameters in this calculation are the products, velocity gradients times layer depth, for each layer through which the ray travels.

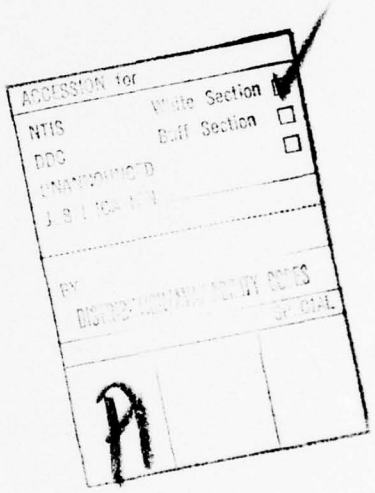

ABSTRACT

Acoustic ray tracing in media where there are velocity gradients is a standard technique for a stationary transmitter and receiver. Also, dealing with moving sources and receivers and with the ensuing Doppler shifts is common practice in the absence of velocity gradients, i.e., when sound ray paths are straight lines. Although calculation of Doppler shifts when sound ray paths are curved are implicit in that part of the literature dealing with the total sound field, some interesting relations remain hidden when the problem is considered in such general terms and only become apparent when the Doppler effect is considered on its own.

Such a study was conducted, its major results being as follows:

1. It is shown that the range rate of the source can be estimated from a knowledge of the transmitted frequency and the angle of the reception of the sound.

2. When there is a vertical offset between source and receiver, the Doppler shift reaches a maximum value at some finite horizontal separation between the two. The equations governing the specific relations are given.

3. It is shown how the error may be calculated when it is assumed that the sound propagates along a straight line rather than along the actual curved ray path. The significant parameters in this calculation are the products, velocity gradients times layer depth, for each layer through which the ray travels.

TABLE OF CONTENTS

LIST OF TABLES

LIST OF FIGURES

LIST OF FIGURES (Continued)

LIST OF SYMBOLS

a	depth difference between the locus of arc center and the receiver
b	vertical extent of a refracted ray in a given layer
c	speed of sound in the medium
c_n	speed of sound in layer n
c_o	speed of sound where a refracted ray is horizontal
c_r	speed of sound at the receiver
c_s	speed of sound at the source
c.p.a.	closest point that an approaching source reaches to an offset receiver
d	depth difference between the locus of ray-arc centers and the source
D	magnitude of Doppler shift
f	frequency of sound
g	sound velocity gradient, assumed in the z (depth) direction
h	total horizontal separation between the source and the receiver or, in the case of an offset receiver, the separation between the source and the c.p.a.
$h_{a,b}$	part of the total horizontal separation
h_n	horizontal distance that a ray travels in layer n
H	actual horizontal separation between the source and the receiver
p	normalized horizontal separation between the source and the receiver
q	normalized vertical receiver offset
R	radius of curvature of a refracted raypath
Rec	indicates the position of a receiver
S	indicates the position of a source

t	period of source travel time
T	travel time along a ray
v_s	velocity of the source
Y	horizontal offset of the receiver from the source path
z	Cartesian coordinate axis which extends in the direction of increasing depth
Z	difference in depth between the source and receiver, referred to as the vertical offset
Δt	period of source travel time
ΔT	difference in travel time between two sound rays
$\Delta\tau$	period of time which the receiver continually receives sound
ϕ	angle formed by the source path and the direct path between the source and the horizontally offset receiver
θ	elevation angle of a refracted ray, formed by a tangent to the ray at the point of interest, and horizontal
θ_1	elevation angle of a ray at its source, referred to as the angle of emission
θ_ℓ	angle of emission of a ray which travels through a series of two or more layers, such that it is the limiting ray of the uppermost layer
θ_{lim}	angle of emission or entrance (to a layer) of that layer's limiting ray
θ_n	elevation angle of a ray where it enters or exits layer n
θ_r	elevation angle of a ray at the receiver, referred to as the angle of reception

ACKNOWLEDGMENTS

The author wishes to express sincere appreciation to his adviser, Professor R. O. Rowlands, for his guidance, patience and clever insight. Gratitude is also extended to the members of the author's defense committee, Dr. Robert W. Farwell and Dr. William Thompson, Jr.

The support of the Applied Research Laboratory at The Pennsylvania State University under contract with the Naval Sea Systems Command is also acknowledged.

CHAPTER I

INTRODUCTION

1.1 The General Problem: Nature and Importance

Doppler shift is the change in the frequency of a sound that is attributed to motion of the source or the observer. Depending on the point of observation and the conditions of the medium, the received Doppler shift is either constant or, more often, time varying. The time varying nature of the phenomenon can cause problems in three major areas. One entails the detection of a pure tone in noise. This can be done by processing the signal and noise by means of a Fast Fourier Transform (FTT) algorithm which performs a frequency analysis of the conglomerate signal. If the resolution of the FFT is great enough, its output will indicate the frequency of the detected pure tone. However, rapid changes in the Doppler shift causes a frequency smearing of the desired (pure tone) signal, resulting in an ambiguous FFT output.

In addition to the time difference between receiver locations, Doppler shift plays an important role in the decorrelation of wideband signals at physically separated receiver positions. This results from the same signal arriving at two different receiver positions carrying two different Doppler shifts. This causes the two received signals to no longer align in frequency.

A third problem arises from SOFAR (Kinsler and Frey, 1962; Officer, 1958) propagation, where a multitude of different Doppler-shifted signals arrive at the receiver during a particular interval of

time. This results in the smearing of the received signal in time and frequency.

1.2 Previous Related Studies

Previous investigations in the area of underwater sound propagation have often employed expressions for Doppler shift. However, these expressions often assume straight-line ray paths, even when the medium under consideration has one or more sound velocity gradients. No investigation to date has specifically approached Doppler shift observed along refracted rays.

Although not directly addressing the Doppler problem, the paper "The Spacing of Underwater Arrays for a Diversity Reception Acoustic Telemetering System," by Rowlands and Quinn (1967), developed many useful relationships which are employed in this study. The intent of their paper was to optimize the spacing between receivers for diversity reception in ocean conditions. The factors they considered include the variation of refracted ray-path lengths with respect to the length of the common direct path.

The following research reports have pursued various aspects of the three Doppler related phenomena mentioned previously. They have treated Doppler shift with varying degree of complexity.

An initial investigation on Doppler-induced degradation of the cross correlation between the outputs of two fixed arrays was reported by Gerlach (1976). In his paper, he presented optimized integrator times which minimize the effects of source motion. One of the drawbacks of this study was the neglect of propagation refraction by sound velocity gradients in the medium.

Sound propagation in the SOFAR channel has been intensively studied by a number of investigators. The report by Jacyna, Jacobson and Clark (1976) developed an analytical approach to the moving, continuous wave source problem in an isospeed channel. They accounted for some source motion by assuming the sound source to be stationary while replacing its frequency with an approximate Doppler frequency. The resulting outputs of two uniform, colinear arrays were then utilized to determine source parameters. The effects of wave refraction and changing source-receiver separation on Doppler shift were not accounted for in that study. In another paper, Jacyna and Jacobson (1977) developed an equation which they claim accurately approximates the gross behavior of cumulative phase. From that result, it was shown that Doppler-shifted frequency at the receiver approaches the conventional Doppler shift of straight-line rays in an isospeed medium. Clark, Flanagan and Weinberg (1974, 1976), in a two-paper series, probed the effect of source movement on coherent multipath. The first paper (1974) used computer modeling to illustrate that constant speed, radial source motion in a deep ocean is a major contributor to transmission fluctuations of both phase and amplitude. It predicated that the Doppler shift along a refracted ray would be slightly different from the conventional Doppler shift. The second paper (1976) clarifies the nature of various multipath spreading effects introduced by source motion. It has established the relative importance of travel-time variations and boundary effects for multipath interference, while treating Doppler shift as a secondary consideration by assuming it to be a constant frequency shift.

In summary, many of the aforementioned papers accounted for Doppler shift to some extent. The coverage ranged from the assumption that Doppler shift is a constant entity that is dealt with by placing the source in a stationary position while replacing its frequency with the Doppler shift frequency, to the assumption that all Doppler shift can be approximated by conventional, straight-line Doppler. The research to date has generally been concerned with the cumulative phase of all signals which reach the receiver. Hence, the effect of wave refraction on Doppler shift has been largely ignored.

1.3 Specific Statement of the Problem

Looking strictly at Doppler-shifted signals which propagate under refractive conditions reveals some interesting relationships between the Doppler shift and the geometry of the source and receiver. The intent of this theoretical study is to bring these relationships to light by exploring their derivation and application in certain typical environments that occur in the ocean. This section will outline the assumptions and conventions followed throughout this study.

Doppler shift is basically the shift in frequency of received sound due to motion of the sound's origin (source) and observer (receiver). When a stationary, spherical source radiates into an infinite, homogeneous medium, successively emitted sound waves radiate concentrically outward. Adding motion to the source results in a loss of this concentricity, such that the wavelengths are compressed ahead of the source motion and expanded behind the source. This compression and expansion of the wavefronts are seen as respectively shorter and longer wavelengths, which alter the frequency of the received signal.

A receiver directly in line with an approaching source detects the full compression of wavefronts. Since the velocity of sound remains constant, the receiver perceives the shortened wavelength as a higher frequency than that produced. Source motion in the direction of the receiver will be considered positive, resulting in positive Doppler shift. Negative Doppler shift is caused by the source movement away from the receiver.

Although Doppler shift is usually described for a moving source with a fixed receiver, a moving receiver with a fixed source provides similar results. A receiver moving toward a stationary source will perceive sound waves with a positive Doppler shift since the movement causes wavefront incidence to occur at shorter time intervals than without movement. The expression for Doppler shift due to a moving receiver is of a form slightly different than that of the moving source. However, as shown in Chapter II, the expressions are essentially equal for source velocities with which we are concerned, which are small compared with the velocity of sound. Hence, the relationships derived and discussed in this paper, when placed in terms of source movement, apply as well to receiver movement.

The effect of Doppler shift can be continuous or changing, depending on the point of observation. Receivers on the source path receive sound of constant frequency shift. Receiver positions not on the source path, but horizontally or vertically offset from it, receive sound which is Doppler shifted to a degree that depends on the offset and the separation from the source. An absence of Doppler shift can be observed only at points which lie perpendicular to the source path, at the source. However, these points experience only an instantaneous lack of Doppler since the source will be moving past the point to which they

are perpendicular. Otherwise, the receiver would have to move at the same velocity as the source. Any point in space with which the source has zero relative motion will receive sound at its true frequency.

In a medium such as the ocean, the velocity of sound changes with depth. This is mainly due to the change of temperature of the medium at shallow depths, and the increase in pressure at large depths (Kinsler and Frey, 1962, p. 471). This change in sound velocity over a given depth span is denoted as the sound velocity gradient (or gradient, for short), and is implied in the direction of increasing depth (along the z-axis; the x- and y-axes extend along the plane which defines the ocean surface, which is assumed to be parallel to the ocean bottom). For purposes of this paper, it is also assumed that the sound velocity is constant along the x and y directions.

When a gradient occurs in the medium, sound is refracted. To observe this refraction, sound rays, which are lines perpendicular to the wavefronts, are used to indicate the direction of refracted energy flow as it propagates. The path that a refracted ray follows is described in the next chapter.

At any given time in an infinite refractive medium, consider one particular ray which leaves the spherically radiating source and intercepts the receiver. This ray follows Fermat's principle of least travel time (Officer, 1958, p. 42). Although source movement is not restricted in any way in this study, discussed movements are mainly in a horizontal plane at the depth of the source since that is of the most practical interest. This causes a continuous change in the ray path which fulfills the Fermat requirement. This change leads to changes in the travel time from the source to the receiver, the angle of ray

emission from the source, and the horizontal source-receiver separation. Closed form expressions of these quantities are sought to define the resultant changes in Doppler shift. This is dealt with in Chapter II, and with further complications in Chapter III. The error in Doppler shift between refracted rays and their straight-line approximations for certain practical situations is the concern of Chapter IV.

The specific purpose of this study is to investigate the effects of constant sound velocity gradients along with differences in source and receiver depths, on the Doppler shifting of continuous wave, acoustic propagation. The results will be compared to propagation in a homogeneous medium.

CHAPTER II

DERIVATION OF DOPPLER EXPRESSIONS

2.1 General Expressions

It is first necessary to obtain a general expression for the Doppler shift in terms of the change in sound travel time that is induced by movement of the source or receiver. A common assumption used in underwater sound propagation is to model the medium as a structure composed of constant velocity-gradient layers (Kinsler and Frey, 1962, p. 466). This model will be used throughout this study except, of course, where noted.

Consider a sound source moving horizontally with velocity v_s toward a fixed receiver. This is represented in Figure 2.1, where two ray paths that are refracted by the gradient intercept the receiver denoted as "Rec". Sound that travels along the second ray path is emitted by the moving source at a time Δt after that which travels along the first path. These ray paths can be considered as representing the beginning and the end of a period of time in which the source continuously emits sound. This sound follows paths that pass through the receiver location. If the times required for the sound to traverse the paths are T_1 and T_2, respectively, then the difference in travel time between these two paths is:

$$\Delta T = T_1 - T_2 \quad .$$

The period of time during which the receiver continually receives sound is given as $\Delta\tau$, where:

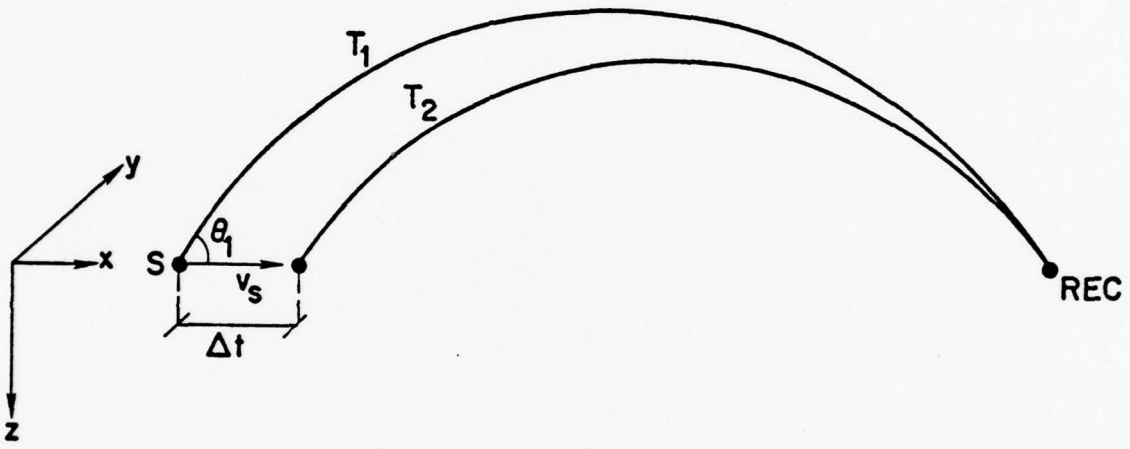

Figure 2.1 Refracted Sound Rays Which are Successively Emitted from a Horizontally Moving Source.

$$\Delta\tau = (\Delta t + T_2) - T_1 = \Delta t - \Delta T \quad .$$

This relationship is valid with the assumption that the source velocity is much less than the speed of sound. This insures that ΔT is smaller than Δt .

During the time interval Δt , the moving source emits $f\Delta t$ cycles of continuous wave sound. These cycles are received during time interval $\Delta\tau$ resulting in an apparent frequency of:

$$f_{apparent} = \frac{f\ t}{(\Delta t - \Delta T)} = f\ \frac{1}{[1 - (\Delta T/\Delta t)]} \quad .$$

When $\Delta T/\Delta t$ is very small, this formula equals:

$$f_{apparent} = f[1 + (\Delta T/\Delta t)] \quad , \qquad (2.1)$$

which is the form for a moving receiver. Thus, the Doppler shift term can be defined as $f(\Delta T/\Delta t)$, which becomes $f(dT/dt)$ as Δt approaches zero.

To apply Equation (2.1) to layered media first requires that the path of sound be defined. For this purpose, it will be assumed that the sound velocity gradient, g, is constant within each layer and that the velocity is continuous at each boundary. By Snell's law, the angle that the ray path makes with the horizontal is the same on each side of the boundary. At any given source location, the ray path that intercepts the receiver will depend on the velocity gradient of each of the layers through which it travels. This path may be defined within a layer by a circular arc of radius R (Figure 2.2), such that:

$$R = \frac{c_o}{g} \quad , \qquad (2.2)$$

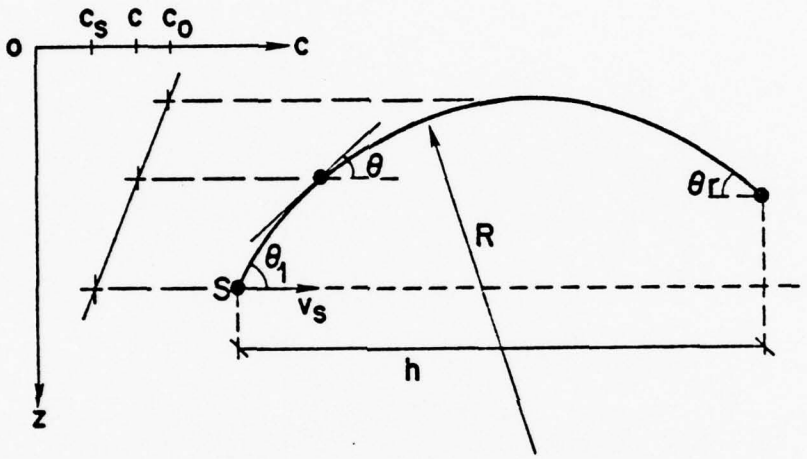

Figure 2.2 Refracted Ray Path Parameters in a Single Layer.

where c_o is the velocity of sound at the depth where the ray would become horizontal. At any other point along the ray path, the speed of sound is related by Snell's Law (Officer, 1958, p. 48) to the elevation angle of the ray, θ (the angle formed by a tangent to the ray at the point of concern with horizontal). This is given as:

$$c = c_o \cos\theta \quad . \tag{2.3}$$

In particular, the speed of sound at the source is:

$$c_s = c_o \cos\theta_1 \quad .$$

This relationship allows further definition of the ray path. In terms of the angle that sound must be emitted at to follow the ray path:

$$R = \frac{c_s}{g \cos\theta_1} \quad .$$

In a multi-layered situation (Figure 2.3), sound entering the n^{th} layer with velocity c_n, and at an angle of θ_n, describes the ray path's radius as:

$$R_n = \frac{c_n}{g_n \cos\theta_n} \quad . \tag{2.4}$$

It has been previously shown by Rowlands and Quinn (1967) that the rate of change in arc radius for a change in emission angle is:

$$\frac{dR}{d\theta} = R \tan\theta \quad .$$

In more useful form:

$$\frac{dR}{R} = \tan\theta \, d\theta \quad . \tag{2.5}$$

They have also shown that dR/R is constant throughout the entire path. Therefore, at the point of origin of a ray path, or at its entrance and exit from a layer, it holds that:

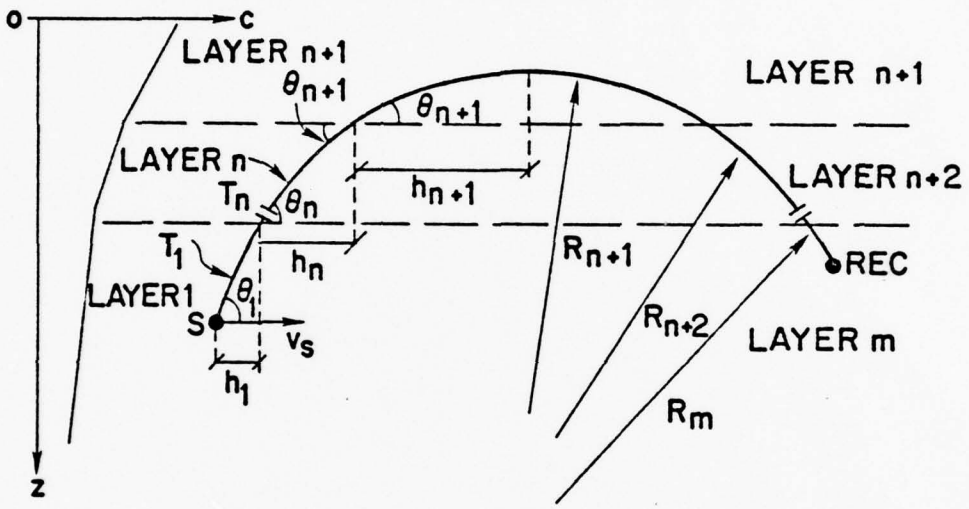

Figure 2.3 Raypath in a Multi-Layered Medium.

$$\frac{dR_n}{R_n} = \tan\theta_1 \, d\theta_1 = \tan\theta_n \, d\theta_n = \tan\theta_{n+1} \, d\theta_{n+1} \quad ,$$

where θ_n and θ_{n+1} are the respective angles of ray entrance and exit to layer n.

It follows that:

$$\frac{d\theta_n}{d\theta_1} = \frac{\tan\theta_1}{\tan\theta_n} \tag{2.6}$$

and

$$\frac{d\theta_{n+1}}{d\theta_1} = \frac{\tan\theta_1}{\tan\theta_{n+1}} \quad .$$

The distance along an arc is equal to the radius times the angle of the arc sector. Since ray paths curve in circular fashion, the velocity along the ray path can be described as the distance traveled per unit of time, or:

$$c = R \frac{d\theta}{dT} \quad . \tag{2.7}$$

Substituting this relationship and that of Equation (2.2) into Equation (2.3) produces:

$$\frac{d\theta}{dT} = g \cos\theta \tag{2.8}$$

or

$$dT = \frac{d\theta}{g \cos\theta} \quad . \tag{2.9}$$

The total travel time is composed of a series of individual travel times that stem from the ray's travel through individual layers. Treating the layers which the sound re-enters on its downward path as separate segments, then, referring to Figure 2.3, there are m segments for which the travel times have to be summed. Thus,

$$T = \sum_n \int_{\theta_n}^{\theta_{n+1}} \frac{d\theta}{g_n \cos\theta} = \sum_n \frac{1}{g_n} \log \frac{1 + \sin\theta}{1 - \sin\theta} \Bigg|_{\theta_n}^{\theta_{n+1}} ,$$

where $1 \leq n \leq m$. This expression can be differentiated with respect to θ_1 to determine the change in total ray path travel time for a change in the angle of emission:

$$\frac{dT}{d\theta_1} = \sum_n \left[\frac{1}{g_n} \sum_n \frac{1}{\cos\theta_n} \frac{d\theta_n}{d\theta_1} - \frac{1}{\cos\theta_{n+1}} \frac{d\theta_{n+1}}{d\theta_1} \right] .$$

Substituting Equation (2.6) into this equation provides the form:

$$\frac{dT}{d\theta_1} = \tan\theta_1 \sum_n \frac{1}{g_n} \left[\frac{1}{\sin\theta_n} - \frac{1}{\sin\theta_{n+1}} \right] . \qquad (2.10)$$

In a similar manner, the horizontal source-receiver separation can be described as a summation of segments. The horizontal component of the ray path in a particular layer is the difference between the projections of the radius, as shown in Figure 2.3. This is governed by:

$$h_1 = R_1 \sin\theta_1 - R_1 \sin\theta_2 .$$

The total horizontal distance is therefore:

$$h = \sum_n R_n (\sin\theta_n - \sin\theta_{n+1}) .$$

With R_n replaced by Equation (2.4), the derivative of h with respect to the angle of emission is:

$$\frac{dh}{d\theta_1} = \sum_n \frac{c_n}{g_n} \frac{\tan\theta_1}{\cos\theta_n} \left[\frac{1}{\sin\theta_n} - \frac{1}{\sin\theta_{n+1}} \right] . \qquad (2.11)$$

The source velocity v_s can be expressed as the change in horizontal separation between source and receiver per unit of source elapsed time:

$$v_s = \frac{dh}{dt} \quad .$$

This can also be written as:

$$v_s = \frac{dh}{d\theta_1} \times \frac{d\theta_1}{dt} \quad . \tag{2.12}$$

Applying Snell's Law,

$$\frac{\cos\theta_n}{c_n} = \frac{\cos\theta_1}{c_s}$$

to the substitution of Equation (2.11) into Equation (2.12) provides:

$$\frac{d\theta_1}{dt} = \frac{v_s}{c_s} \frac{\cos\theta_1}{\tan\theta_1} \sum_n \frac{g_n}{\left[\frac{1}{\sin\theta_n} - \frac{1}{\sin\theta_{n+1}}\right]} \quad . \tag{2.13}$$

Finally, since

$$\frac{dT}{dt} = \frac{dT}{d\theta_1} \times \frac{d\theta_1}{dt} \quad ,$$

an expression for Doppler shift along a refracted ray in any constant gradient layer will result from the multiplication of Equation (2.13) by Equation (2.10). The terms involving the angles of layer interfaces all cancel leaving the magnitude of Doppler shift, D , where:

$$D \equiv f \frac{dT}{dt} = f \frac{v_s \cos\theta_1}{c_s} \quad . \tag{2.14}$$

This relationship expresses the Doppler shift as simply the projection of the source velocity in the direction of a ray path divided by the sound speed at the source. It follows that any source movement that will not project along a receiver-bound ray (i.e., source movement

perpendicular to the ray at ray emission) will not contribute to the Doppler shift seen along that path.

Substituting Snell's Law into Equation (2.14) allows the Doppler shift to be found at any point along the ray path. The usefulness of this result shows when the speed of sound and the magnitude of the Doppler shift are determined at the receiver. This information supplies all that is needed to calculate the horizontal velocity of the source as it travels toward the receiver.

2.2 Single Layer Summations

Sound velocity gradients in a medium refract the sound as it travels in a manner that forces the sound ray toward depths of slower sound speed. A negatively sloped gradient bends an upward going ray (i.e., in the direction of increasing sound speed) such that its direction of propagation changes from upward to horizontal. Once horizontal, the ray has reached minimum depth and maximum sound speed, designated c_o, before starting its downward travel. A similar process takes place for a downward going ray in a positively sloped gradient. Illustrated in Figure 2.4 are a positive and a negative gradient, each of which are represented by linear approximations. Also shown are two refracted rays, each of which are emitted partially in the direction of increasing sound speed. Situations like this, where positive and negative sloped gradients meet at a sound speed maximum, form the basis for a SOFAR axis.[1]

---

[1]For a complete description of SOFAR propagation, see Kinsler and Frey, 1962, p. 471, and Officer, 1958, p. 100.

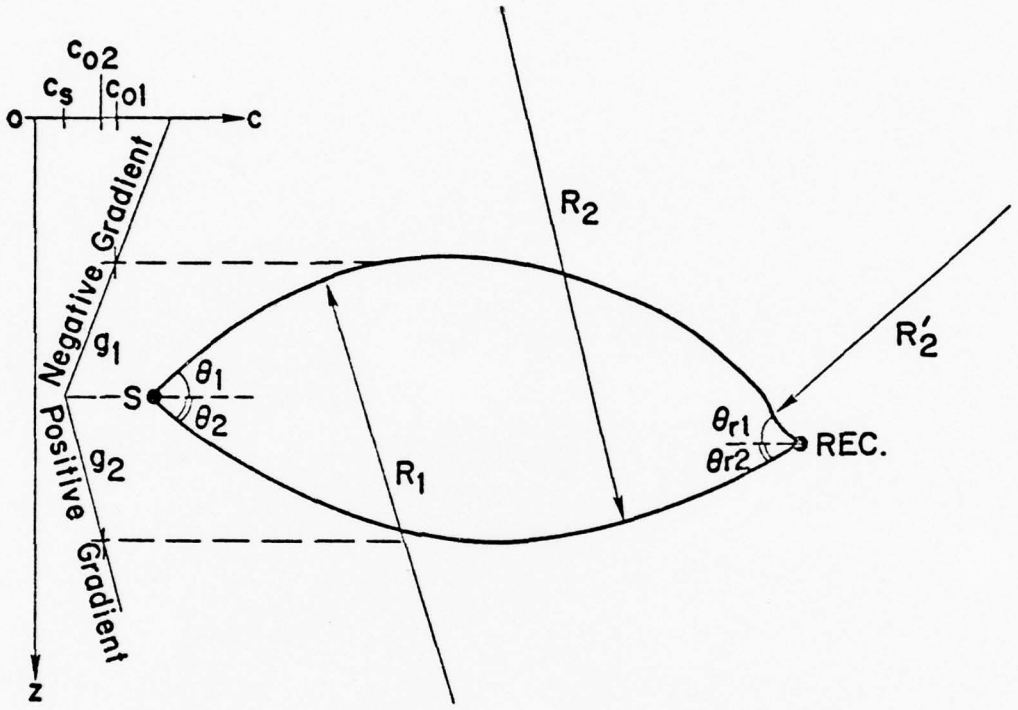

Figure 2.4 Positive and Negative Sound Velocity Gradients (Which Meet at a Sound Velocity Minimum) with Typical Rays.

Consider propagation through a single linear velocity gradient (one layer). Summations for horizontal separation and travel time are taken from the angle of emission to the angle of reception. However, since the point of reception can be made anywhere along the ray path, the angle measured from the horizontal of a ray tangent at the receiver, θ_r, can take on any value from -90^o to 90^o. Should the ray reach its horizontal position before intercepting the receiver, then provision must be made for the resultant change of sign that θ_r undergoes. This is easily accounted for by splitting the summations into two parts. One part covers the range from $\theta = \theta_1$ to $\theta = 0^o$ (angle of ray elevation at horizontal), while the other is summed from $\theta = 0^o$ to $\theta = \theta_r$. For the special case where the source depth equals that of the receiver, part one equals part two and θ_1 equals θ_r. This allows expressions for travel time and horizontal distance to simply be twice that found in summing over the θ_1 to 0^o interval.

2.3 Effect of Boundary Reflections on Doppler Shift

Summation terms have been expressed for n layers of ray travel. Each layer has been described in terms of the ray path's entrance and exit angles. Since these summations are carried out over the entire path of a receiver-intercepting ray, radical changes in the slope of the gradient (for instance, positive to negative slope transitions) must be accounted for. This flexibility forms the basis for adaptation to boundary reflections.

Consider a ray which is incident on a smooth pressure release surface at an angle of θ_n. The ray is reflected downward at an angle equal to θ_n as shown in Figure 2.5. The situation may be represented as a continuation of the medium above the surface, with the velocity

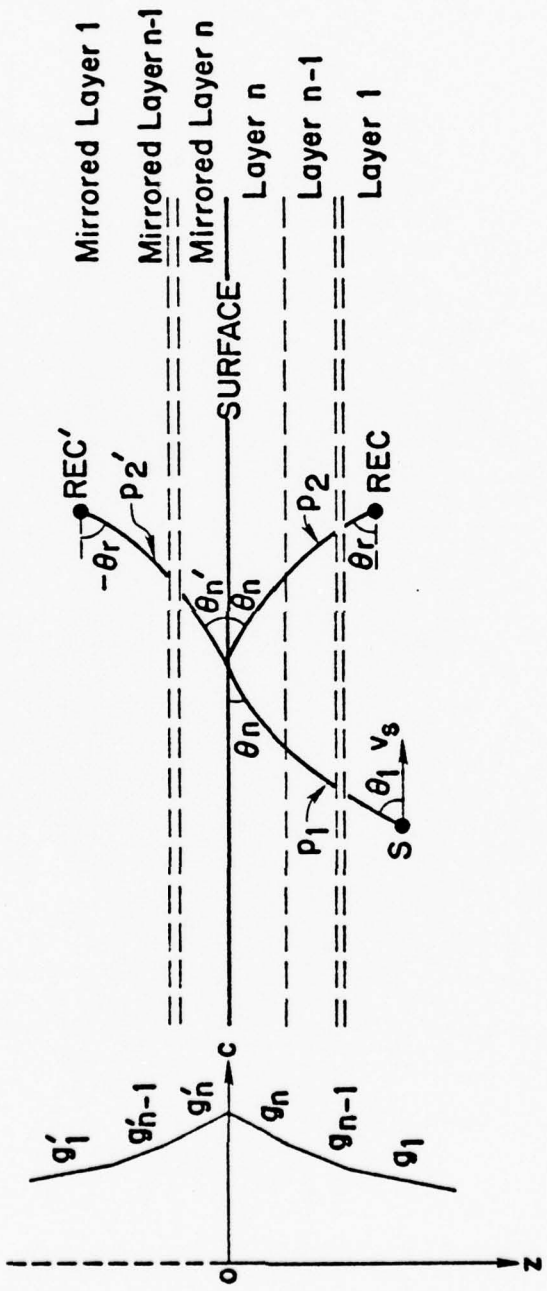

Figure 2.5 Treatment of Reflecting Boundaries.

gradients being the mirror image of those below the surface. Consistent with this is the premise that sound travels from the source through a series of linear gradient layers, become incident on the boundary interface, and continues through an additional series of image layers to the image receiver. The path p_2' which extends from the boundary interface to the image receiver is the mirror image of the actual reflected path p_2. The angle that p_2' forms with the interface θ_n' is therefore identical to that which p_2 forms (the angle of reflection from the boundary). It is well known that the angle of reflection equals the angle of incidence. Therefore, θ_n (the angle of a ray exiting layer n) equals θ_n' (the angle of the ray entering the mirrored layer n').

When the source and receiver are at the same depth, the angle of reception equals the angle of emission as it did in the single layer situation mentioned previously. This makes p_2 and therefore, p_2' equal to p_1, such that summations for p_1 (from θ_1 to θ_n) can be doubled to account for the entire ray path. Vertically offset receivers, however, will require summations from θ_1 to θ_n and θ_n' to θ_r'.

CHAPTER III

DOPPLER VERSUS RANGE FOR PARTICULAR GEOMETRIES

3.1 Differences in Doppler Shift Between Refracted and Non-Refracted Rays

The simplest case of Doppler shift occurs in a homogeneous medium where the source approaches a receiver that is in line with the source's trajectory. To intercept the receiver, the ray must leave the source in line with the source velocity causing the acoustic wavelength to be fully compressed. This results in a Doppler shift that remains at a constant, maximum magnitude for the entire period of source approach. This is shown in Figure 3.1, where the magnitude of Doppler shift is plotted against the normalized horizontal separation between the source and the receiver, $\tilde{h}$. Once the source meets and passes the receiver, the source velocity reverses direction with respect to the receiver causing fully expanded wavelengths of sound to reach the receiver. This produces maximum, negative Doppler shift. Hence, the receiver experiences an abrupt positive to negative transition in the Doppler shift of sound it receives.

As stated in Equation (2.4), the curvature of a ray path is dependent on the gradient, the speed of sound, and the angle of ray emission. This is represented in Figure 3.2 for a receiver in line with the source trajectory. Since the gradient is in the depth direction, the speed of sound throughout the horizontal plane at a given depth is constant. Therefore, a horizontally traveling sound source encounters the same gradient and sound speed throughout its movement. This maintains c/g as constant, hereafter denoted as d , which defines

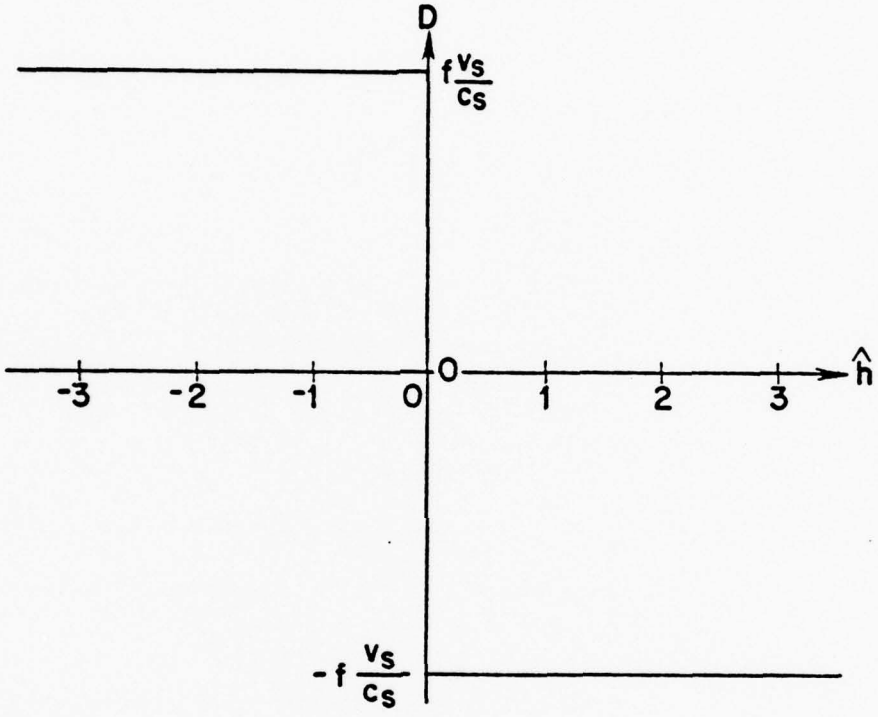

Figure 3.1 Magnitude of Doppler Shift for a Receiver in Line with the Source, in a Homogeneous Medium.

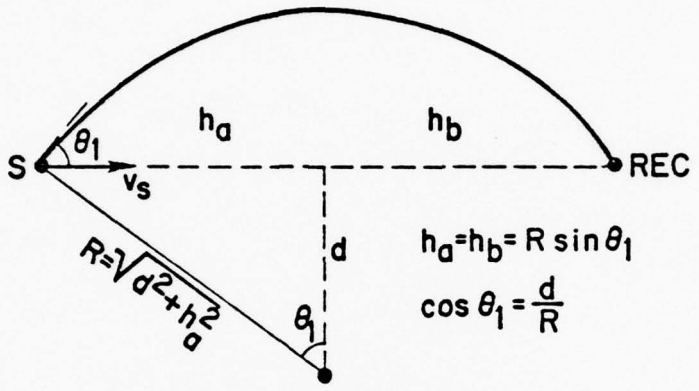

Figure 3.2 Geometric Representation of a Refracted Ray.

the depth of the locus of ray-arc centers below the source trajectory. From Equations (2.2) and (2.3):

$$\cos\theta = \frac{d}{R} \quad , \tag{3.1}$$

which sets d equal to the radius of curvature of the ray that leaves the source horizontally (angle of emission is zero). Equation (3.1) is used to relate half of the horizontal source-receiver separation to the angle of ray emission:

$$\cos\theta = \frac{d}{(d^2 + h_a^2)^{1/2}} \quad . \tag{3.2}$$

Normalizing the depth of arc centers to unity allows the magnitude of Doppler shift (previously derived as proportional to the cosine of the emission angle) to be expressed as:

$$D = f \frac{v_s}{c_s} \frac{1}{(1 + h_a^2)^{1/2}} \times h_a \neq 0 \quad . \tag{3.3}$$

This function is continuous in the vicinity of zero horizontal separation. However, due to the source-velocity direction reversal, the plot of the function versus the horizontal separation (normalized by d) in Figure 3.3 shows a positive to negative transition at $\hat{h}_a$ equal to zero.

The projection of source-velocity along a ray translates into the extent of wavelength compression (or expansion) and, therefore, the Doppler shift seen along the ray [see Equation (2.14)] . At very large distances from the receiver (on the same order of magnitude as the radius of curvature), rays which intercept the receiver are emitted at very large angles; as a consequence, the projections of source velocity along these rays are small. This is consistent with Figure 3.3, where

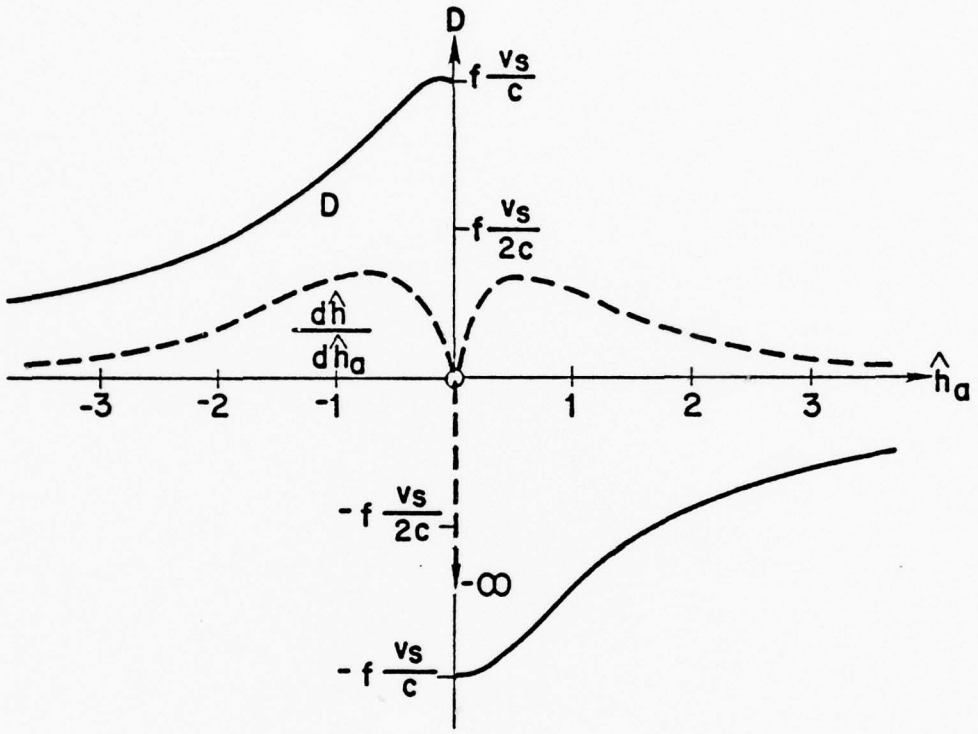

Figure 3.3 Magnitude and the Derivative of Doppler Shift for a Receiver in Line with the Source in a Refractive Medium.

small magnitudes of Doppler shift are shown for large values of $\hat{h}_a$. As the source approaches the receiver, the angle of emission progressively diminishes. This corresponds to an appropriate increase in Doppler shift seen along the ray. Very close to the receiver, intercepting ray paths are very short, traveling an almost straight path (due to a relatively large radius of curvature). These rays are also nearly horizontal, since they are emitted at very small angles. The projection of the source-velocity along these rays results in a large Doppler shift.

The amount of change in Doppler shift for a change in horizontal separation is found by taking the derivative of Equation (3.3) with respect to $\hat{h}_a$. This is given as:

$$\frac{dD}{d\hat{h}_a} = - f \frac{v_s}{c_s} \frac{\hat{h}_a}{(1 + \hat{h}_a^2)^{3/2}} \quad . \tag{3.4}$$

This relationship is defined as $\hat{h}_a$ equal to 0^+ and 0^-, but reflects the Doppler transition by becoming infinite at $\hat{h}_a$ equal to exactly zero. Simply stated, the slope of a vertical line is infinite. This Doppler curve derivative is plotted against $\hat{h}_a$ in Figure 3.3 as a dashed curve. The point of maximum rate of Doppler change occurs at a normalized horizontal separation of 0.7125.

3.2 Doppler Shift for Vertically Offset Receivers

The next consideration is of a source traveling horizontally through a homogeneous medium, past a receiver that is vertically offset from the source trajectory (Figure 3.4a). With an approaching source, successively emitted rays have decreasing travel-time requirements in propagating from the source to the receiver. The emission of two

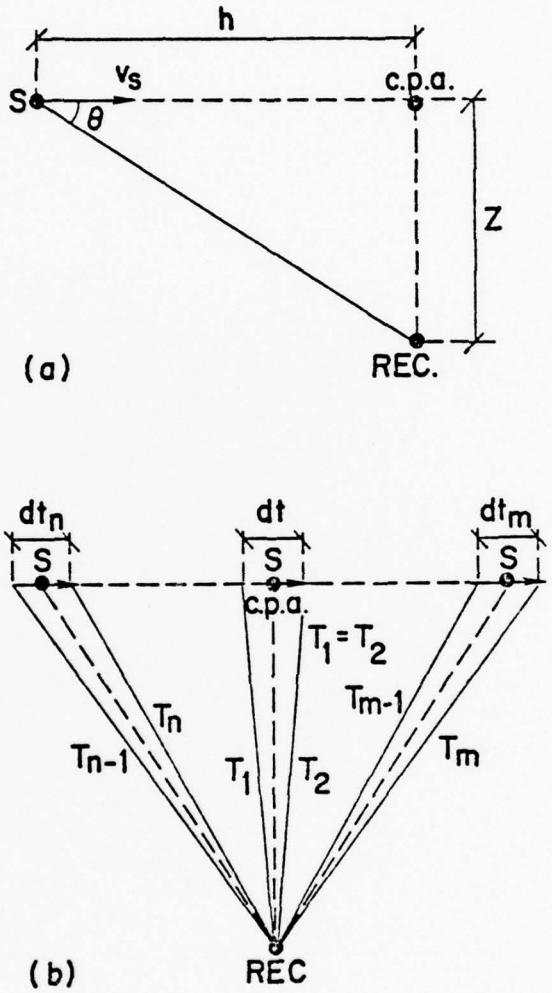

Figure 3.4 (a) Side View of a Vertically Offset Receiver in a Homogeneous Medium.

(b) Straight-Line Rays to a Vertically Offset Receiver Emitted in the Vicinity of the c.p.a.

consecutive rays, such as T_{n-1} and T_n in Figure 3.4b, define the period of source travel time dt_n. Due to the difference in travel time between these two rays, the receiver perceives the dt_n period as shortened in time, thereby as positively Doppler shifted sound. Further approach of the source reduces the travel time difference between rays, subsequently reducing the magnitude of Doppler. In the vicinity of the source's closest point of approach (c.p.a.) to the receiver, as shown in Figure 3.4b, the two sound rays that define the beginning and the end of a period of source travel time (dt) are symmetrically positioned about the c.p.a. This symmetry requires that rays T_1 and T_2 be equal and without a time difference between them. Since there is no change in dT for a change in dt, the receiver perceives the true emitted frequency.

Once the source is past the c.p.a., successively emitted rays require increasingly longer travel time to reach the receiver. This results in a negative dT which is perceived at the receiver as a shift to lower frequency than that produced.

The magnitude of Doppler shift seen at the receiver in this situation is proportional to the ratio of the receiver offset, Z, to the horizontal separation, such that:

$$\theta = \tan^{-1}\left(\frac{Z}{h}\right) \quad ,$$

where

$$\cos\theta = \frac{h}{(Z^2 + h^2)^{1/2}} \quad .$$

With Z normalized to unity, the Doppler magnitude, plotted in Figure 3.5, is described by:

$$D = \pm f \frac{v_s}{c_s} \frac{\hat{h}}{(1 + \hat{h}^2)^{1/2}} \quad . \qquad (3.5)$$

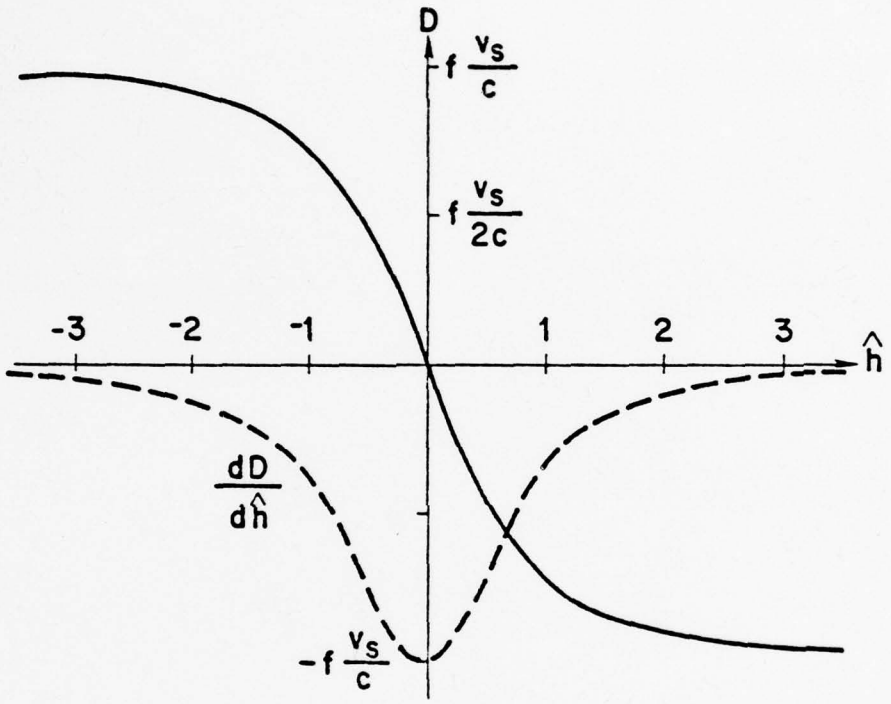

Figure 3.5 Magnitude of Doppler for a Vertically Offset Receiver in a Homogeneous Medium.

From this, the change in Doppler for a change in horizontal separation is:

$$\frac{dD}{d\hat{h}} = \pm f \frac{v_s}{c_s} \frac{1}{(1 + \hat{h}^2)^{3/2}} \quad . \tag{3.6}$$

This is plotted in Figure 3.5 against the horizontal separation normalized by Z .

In a refractive medium, the nomenclature faster or slower offset will be used to denote the position of the receiver with respect to the source trajectory. When a receiver is positioned at a depth where the sound speed is greater than that of the source, it is considered to be a faster offset. A slower offset refers to receiver positions located at sound speeds that are less than that at the source.

The addition of a receiver offset to propagation through a refractive medium can be represented by the configurations illustrated in Figures 3.6 and 3.7. An initial observation that can be made from Figure 3.6 is that there is a point at some horizontal distance away from the receiver from which a receiver-intercepting ray leaves the source in line with the source's horizontal velocity component. At that point, designated as S , the sound emitted in the direction of the ray will be maximally Doppler shifted. Positions previous to and after this point, represented by S' and S'', respectively (also in Figure 3.7), will have magnitudes of Doppler shift that are less than maximum.

An additional comment can be made of Figure 3.6, where a receiver-intercepting ray leaves the source position designated as S' . The ray travels along a path that takes it through another possible

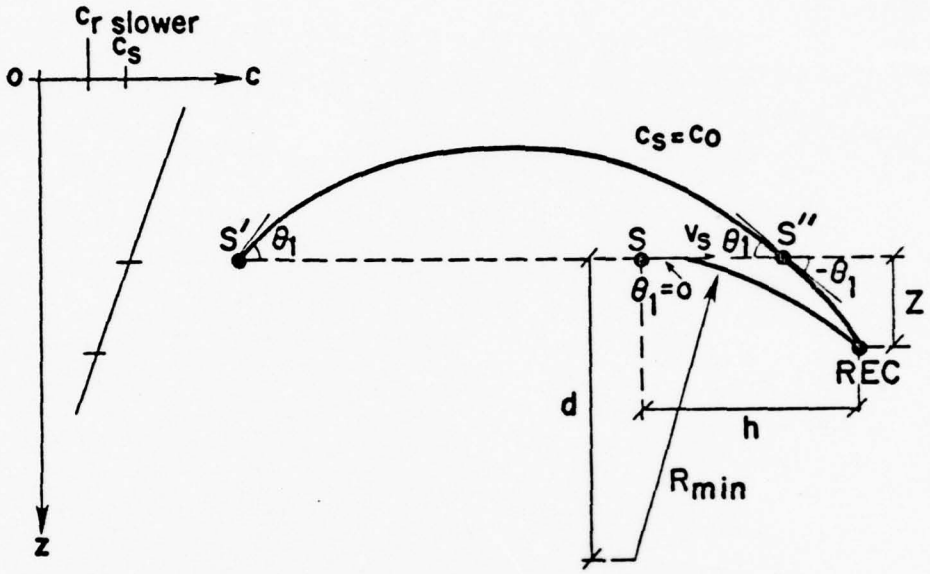

Figure 3.6 Receiver Vertically Offset from the Source Path at a Depth of Slower Sound Velocity than the Source.

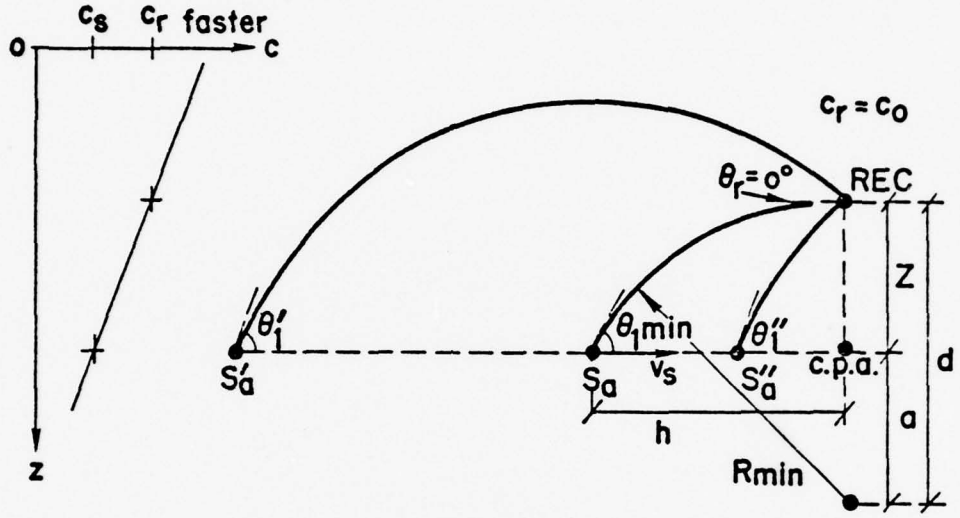

Figure 3.7 Receiver Vertically Offset from the Source Path at a Depth of Faster Sound Velocity than the Source.

source position, S", before reaching the receiver. For a single velocity gradient, there is only one refracted ray that does this.

Because of this, a receiver-intercepting ray emitted at S" must be congruent with the segment of the S' emitted ray that passes through S" and the receiver. Also, since the two source positions are at the same depth, a tangent to the ray path at S" will form an elevation angle of the same number of degrees as a tangent at S' . It follows that the angle of emission of the ray emitted at S" , although measured as negative, is of the same magnitude as the angle of emission at S' . Since the cosine of a negative angle equals the cosine of a positive angle, the magnitude of projected source-velocity and therefore the magnitude of Doppler shift are the same for rays emitted at these two source positions. This is illustrated by an approximate magnitude of Doppler curve, plotted in Figure 3.8. When the source is directly over the receiver, the horizontal separation is zero. At this point (for reasons outlined in the non-refracted ray, offset receiver section), the receiver will not perceive a difference in ray travel time for a change in source travel time. This accounts for the ordinate crossing of the curve that represents the magnitude of Doppler shift in Figure 3.8.

A complementary situation occurs when the receiver has a faster vertical offset (Figure 3.7). As the source approaches the receiver, the angle of emission required by a ray to intercept the receiver diminishes until a ray reaches the receiver horizontally. This point corresponds to a source position (designated as S_a in Figure 3.7) where the ray emission angle is the smallest that can be obtained for this configuration. The magnitude of this minimum angle depends on the

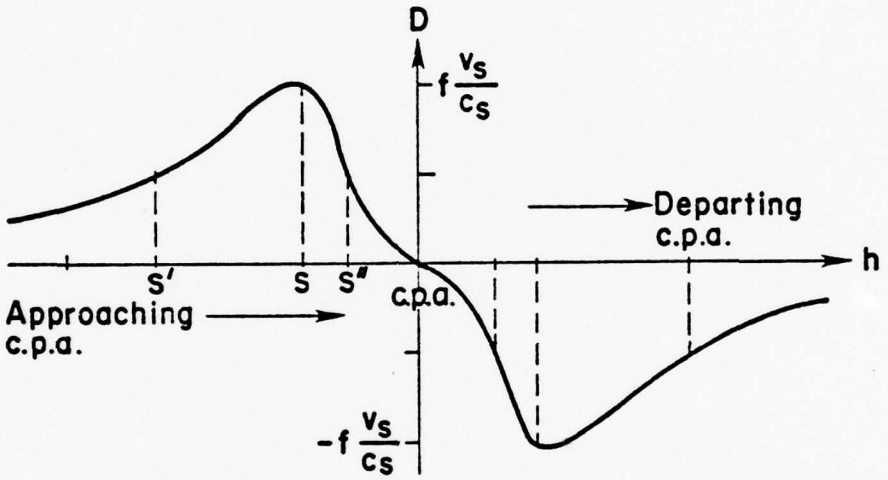

Figure 3.8 Approximate Magnitude of Doppler Curve for a Slower-Offset Receiver.

receiver offset Z such that:

$$\theta_{min} = \cos^{-1}\left(\frac{a}{d}\right) \quad ,$$

where

$$a = d - Z \quad \text{and} \quad d = R_{min} \quad .$$

For a source movement towards the c.p.a., the emission angle initially decreases. This increases the magnitude of Doppler seen at the receiver since Doppler observed along a ray depends on the ray's source-velocity projection. This continues until a maximum is reached at the minimum-angle source position, S_a . Further movement toward the c.p.a. results in the magnitude tapering off to zero (at the c.p.a.). Movement beyond the c.p.a. induces Doppler such that the plot of magnitude versus normalized separation forms an odd function with the pre-c.p.a. plot (Figure 3.8).

The projection of the source velocity along the ray where the Doppler is maximum in the faster offset is less than that which projects along the ray's counterpart in the slower offset configuration. This results in unequal, maximum Doppler magnitudes from which the respective Doppler curves (Figures 3.8 and 3.9) are scaled. Although the magnitude of maximum Doppler can be measured at any point along the ray (by using the angle of a ray tangent at the point), the most convenient (for scaling of the Doppler curves) is that taken at the point where the ray is horizontal. This is applied to the two Doppler curves for offset receivers; Figure 3.8 shows the Doppler scale in terms of source velocity divided by the speed of sound at the source. For Figure 3.9, the ratio is in terms of the speed of sound at the faster offset receiver,

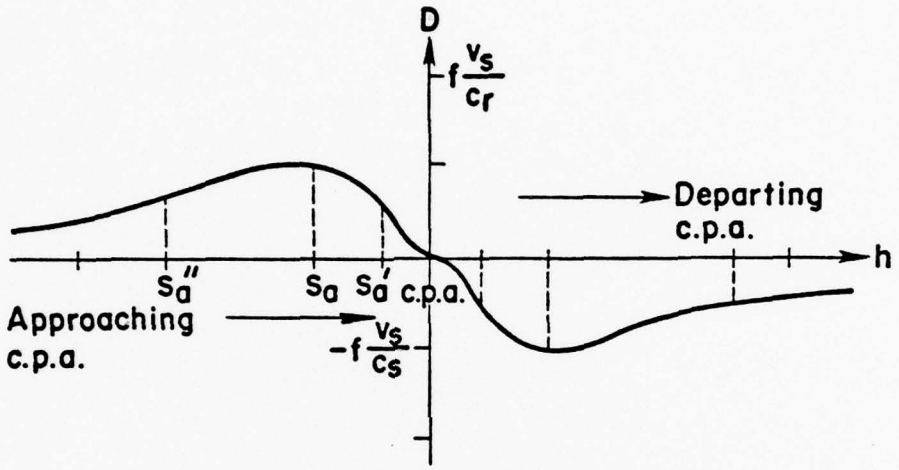

Figure 3.9 Approximate Magnitude of Doppler Curve for a Faster-Offset Receiver.

resulting in a maximum Doppler magnitude that is less than the maximum of the slower offset by a factor of $c_s/c_{r_{faster}}$.

Despite the scaling (which can be alleviated by shifting the faster offset configuration in depth, so that $c_{r_{faster}}$ will equal the original c_s), the two Doppler curves follow the same mathematical expression. This is consistent with the notation which previously defined the source and receiver positions as reciprocal.

The function which the two offset receiver curves follow is dependent on the offset of the receiver and the gradient of the medium. This is derived with respect to the geometric configuration illustrated in Figure 3.10.

The radius of curvature, R, can be described by means of the Pythagorean theorem to equal:

$$R^2 = h_a^2 + d^2 \quad ,$$

where h_a is the horizontal distance traversed by the part of the ray that travels in the direction of increasing sound speed; likewise, it can be expressed as:

$$R^2 = h_b^2 + a^2 \quad ,$$

where h_a is the horizontal distance traveled by the segment of the ray in the direction of decreasing sound speed.

The variable a is the difference in depth between the locus of arc centers and the receiver offset, such that:

$$a = d - Z \quad .$$

The entire horizontal separation between the source and receiver h can now be expressed as:

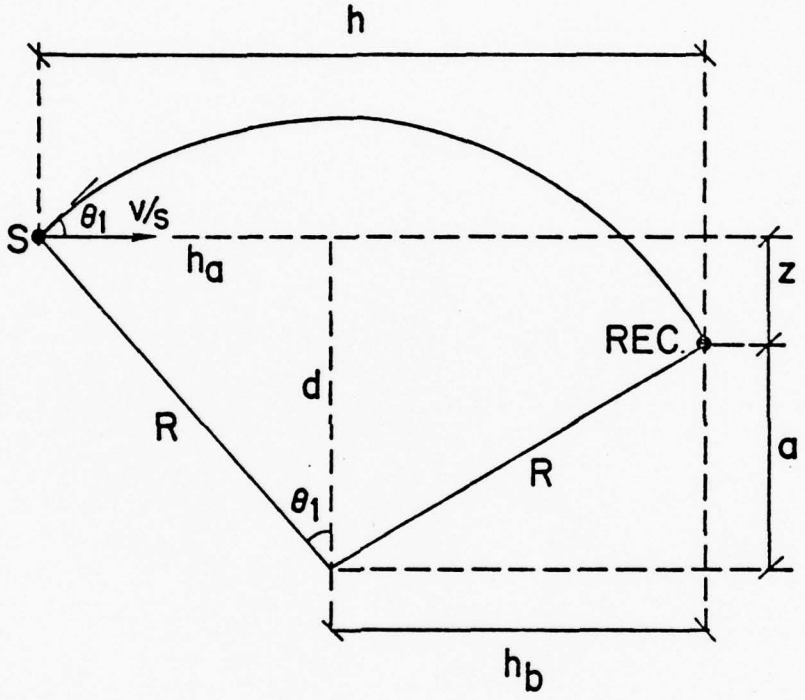

Figure 3.10 Geometric Representation of a Refracted Ray Path to a Vertically Offset Receiver.

$$h = h_a + h_b = \sqrt{R^2 - d^2} + \sqrt{R^2 - a^2} \quad .$$

Squaring both sides provides:

$$h^2 = 2R^2 - a^2 - d^2 + 2\sqrt{R^2 - d^2}\,\sqrt{R^2 - a^2} \quad .$$

Substituting

$$k = h^2 + a^2 + d^2$$

makes

$$k - 2R^2 = 2\sqrt{R^2 - d^2}\,\sqrt{R^2 - a^2} \quad .$$

Squaring both sides produces:

$$k^2 - 4kR^2 = 4a^2d^2 - 4a^2R^2 - 4d^2R^2$$

and

$$k^2 - 4a^2d^2 = 4R^2(k - a^2 - d^2) \quad ,$$

so that by replacing k with its equivalent:

$$k^2 - 4a^2d^2 = 4h^2R^2$$

or

$$\frac{1}{R^2} = \frac{4h^2}{k^2 - 4a^2d^2} \quad . \tag{3.7}$$

Doppler shift has previously been defined as being proportional to the cosine of the emission angle. This provides the impetus for multiplying Equation (3.7) by d^2, such that:

$$\cos^2\theta_1 = \frac{d^2}{R^2} = \frac{4h^2d^2}{k^2 - 4a^2d^2} \quad .$$

Consequently, by replacing k with its equivalent and factoring out the term a^2d^2,

$$\cos^2\theta_1 = \frac{4h^2/a^2}{(h^2/ad + a/d + d/a)^2 - 4} \quad . \tag{3.8}$$

Normalizing with respect to a proves to be a very convenient approach for further simplification of the expression. This normalization results in some new variables defined as:

offset-normalized horizontal separation, $p = h/a$

normalized receiver depth offset, $q = d/a$

such that:

$$p/q = h/d \quad .$$

Supplanting these normalized variables into Equation (3.8) provides:

$$\cos^2\theta_1 = \frac{4p^2}{(p^2/q + 1/q + q)^2 - 4} \quad .$$

Taking the square root of this expression provides one that is directly proportional to the Doppler shift:

$$D \sim \cos\theta_1 = \frac{2p}{\sqrt{(p^2/q + 1/q + q)^2 - 4}} \quad . \qquad (3.9)$$

Figure 3.11 shows this Doppler magnitude equation plotted against the normalized horizontal separation for three values of normalized offset q . The substitution of:

$$m = (p^2/q + 1/q + q)$$

into Equation (3.9) provides much simpler expression of Doppler:

$$D \sim \frac{2p}{(m^2 - 4)^{1/2}} \quad . \qquad (3.10)$$

Since the Doppler shift is dependent on the normalized horizontal separation, the rate by which the Doppler changes as a function of this separation is devised. This is ascertained from the derivative of Equation (3.10) with respect to p , such that:

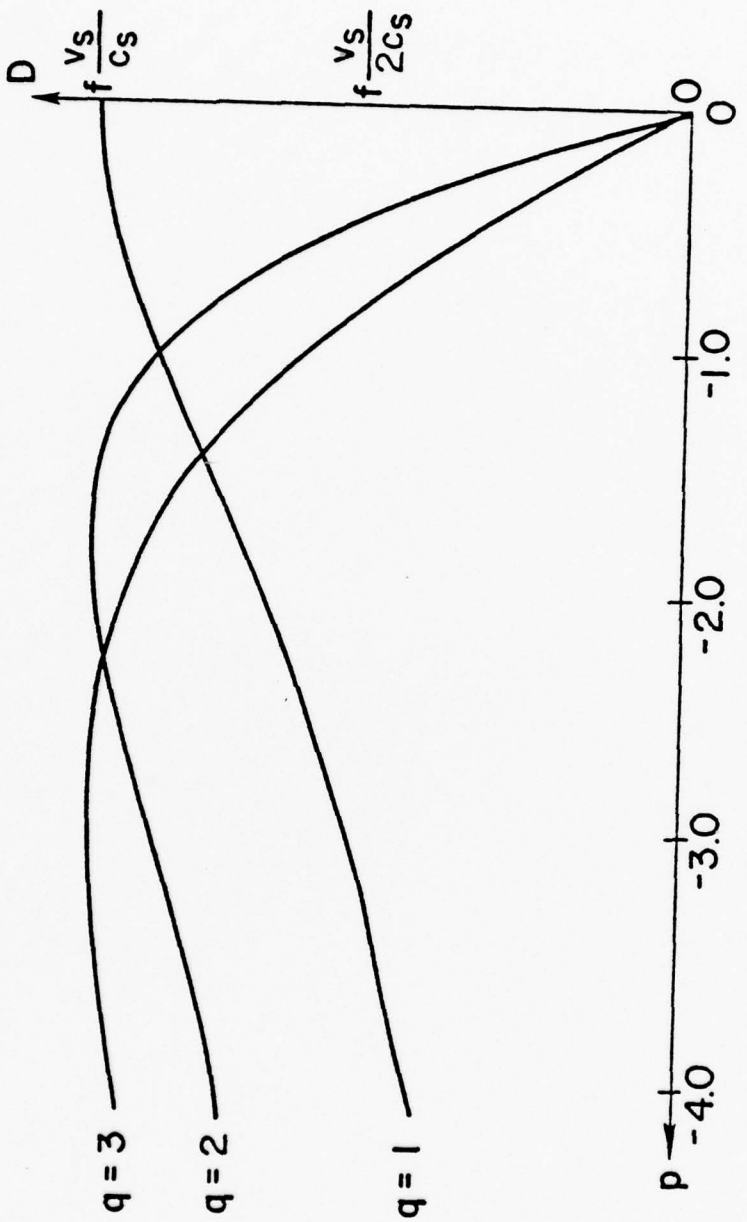

Figure 3.11 Magnitude of Doppler Plotted for Three Values of Normalized Offset.

$$\frac{dD}{dp} = \frac{2[(m^2 - 4) - 2m(p^2/q)]}{(m^2 - 4)^{3/2}} \quad . \tag{3.11}$$

This has been plotted in Figure 3.12 as a function of the normalized horizontal separation for three values of q .

From classical calculus, the derivative of a function is zero at that function's minimum and maximum points. This allows the relationship between the normalized horizontal separation and the normalized receiver offset to be found for the condition of maximum Doppler shift. These points also correspond to zero rate of change of Doppler. From Equation (3.11),

$$\frac{dD}{dp} = 0 \quad ,$$

when

$$m^2 - 4 = 2(p^2/q)m \quad .$$

Substituting in for m provides:

$$2p^2/q = \frac{p^4/q + 2p^2/q^2 + 2p^2 + 1/q^2 + q^2 - 4}{p^2/q + 1/q + q}$$

or

$$p^4/q^2 = (q - 1/q)^2$$

and

$$p^2/q = q - 1/q \quad .$$

Finally,

$$p = (q^2 - 1)^{1/2} \quad . \tag{3.12}$$

This has been plotted in Figure 3.13 and represents the horizontal separation between a source and a receiver required to achieve maximum Doppler shift for a particular receiver depth offset.

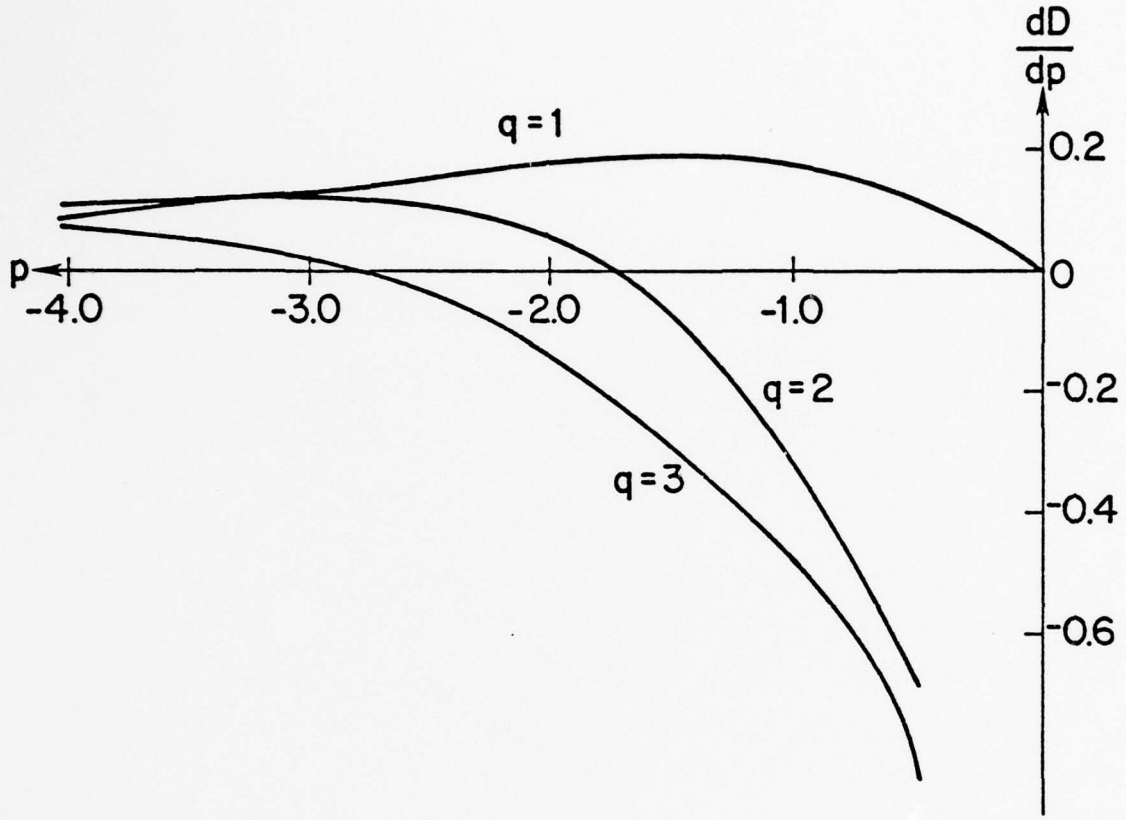

Figure 3.12 Derivative of Doppler Plotted for Three Values of Normalized Offset.

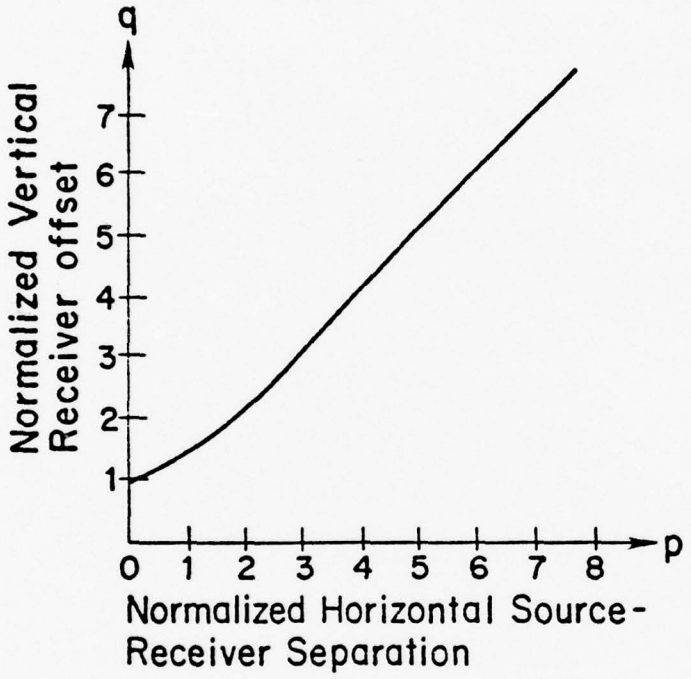

Figure 3.13 Relationship Between the Vertical Receiver Offset and the Horizontal Source-Receiver Separation for Maximum Doppler in a Refractive Medium.

3.3 Doppler Shift for Horizontally Offset Receiver

A horizontally traveling source may pass a receiver that is horizontally offset from the source path by a distance Y (see Figures 3.14a and 3.14b). If this occurs in a non-refracting medium, the horizontal receiver offset will produce the same effect on the Doppler shift seen at the receiver as a vertical receiver offset, assuming that the two offset distances are of equal magnitude. Therefore, the Doppler curve (Figure 3.5), discussion, and equations presented earlier in this chapter (Section 3.2) are valid for a horizontal offset once Z is replaced by Y.

When a horizontal offset is introduced to a receiver in a refractive medium, the expressions for Doppler shift take on increased complexity. Since the sound velocity gradient produces refraction in the depth direction, there is no lateral refraction of the ray. Therefore, receiver-intercepting rays that leave the source at a particular source position will be confined to the plane that extends vertically from a straight line drawn horizontally between the source and the receiver. This straight line (or ray trace) meets the source trajectory at an angle of ϕ, such that part of the source velocity projects along this line. The magnitude of this projection, which is the only factor in the non-refracted, receiver-offset Doppler, is dependent on the cosine of ϕ. Since this ϕ is a function of source position, it may be expressed in terms of the configuration geometry (Figure 3.14a) so that:

$$\phi = \tan^{-1} (Y/h) \quad ,$$

where h is the horizontal separation between the source and the c.p.a.

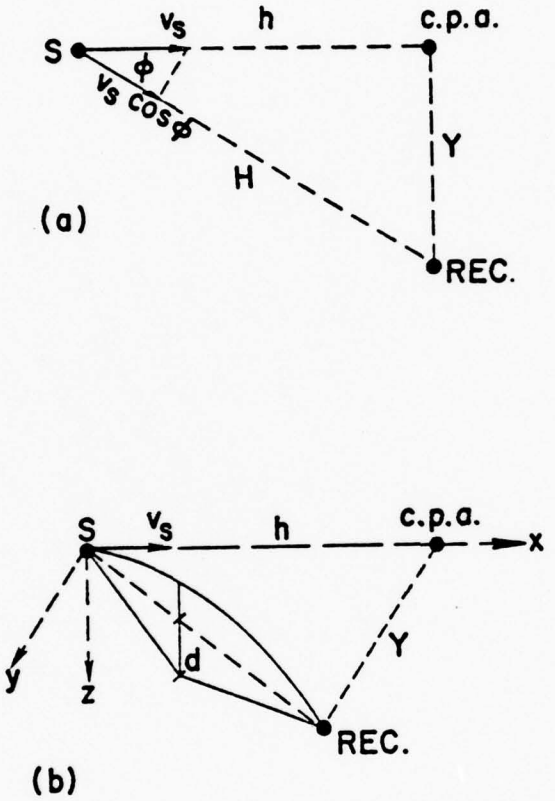

Figure 3.14 (a) Overhead View of a Horizontally Offset Receiver in a Homogeneous Medium.

(b) Orthographic Projection of a Horizontally Offset Receiver in a Refractive Medium.

The source velocity projection is thereby proportional to:

$$\cos\phi = \frac{h}{(Y^2 + h^2)^{1/2}} \quad . \tag{3.13}$$

However, in addition to the offset angle dependence, the source velocity projection depends on the angle of ray emission, since a ray passing from the source to the receiver undergoes refraction. This is illustrated in Figure 3.14b. Hence, the Doppler shift seen along the ray is:

$$D = f\frac{v_s}{c_s}\cos\theta \times \cos\phi \quad , \tag{3.14}$$

or, by substituting in with Equation (3.13) and applying Equation (3.2):

$$D = f\frac{v_s}{c_s} \times \frac{d}{(d^2 + H^2)^{1/2}} \times \frac{1}{(1 + Y^2/h^2)^{1/2}} \quad , \tag{3.15}$$

where H represents the true horizontal separation between the source and the receiver. From Figure 3.14a,

$$H = (h^2 + Y^2)^{1/2} \quad .$$

The latter two terms of Equation (3.15) are related in a somewhat inversely proportional manner, such that the cosine of the offset angle decreases while the cosine of the emission angle increases as the source approaches the c.p.a. (for a constant offset distance). This conglomeration reaches a maximum only for optimum combinations of Y and h (d is normally a constant that depends on medium characteristics).

A desirable relationship to know is one that will provide the receiver offset and horizontal separation combinations that will produce maximum Doppler shift. This is obtained by first finding the change in

Doppler for the source-movement-induced change in horizontal separation. That is:

$$\frac{dD}{dh} = f\frac{v_s}{c_s}\left[\frac{1}{(1 + H^2/d^2)^{1/2}} \times \frac{1}{(1 + Y^2/d^2)^{1/2}} \times \left\{\frac{Y^2}{h^3(1 + Y^2/h^2)} - \frac{h}{4d^2(1 + H^2/d^2}\right\}\right] .$$

The importance of this derivative becomes evident when it is set equal to zero (for the maximum/minimum Doppler condition). This gives:

$$\frac{Y^2}{h^3(1 + Y^2/h^2)} - \frac{h}{4d^2(h^2/d^2 + 1)} = 0 ,$$

from which the desired relationship is algebraically derived to be:

$$h = Y^{1/2}(4d^2 + Y^2)^{1/4} .$$

To simplify this equation, it can be normalized by d which is a constant. This results in normalized variables of $\hat{Y}$ and $\hat{h}$ which are related by:

$$\hat{h} = \hat{Y}^{1/2}(4 + \hat{Y}^2)^{1/4} . \qquad (3.16)$$

This relationship, as plotted in Figure 3.15, provides the horizontal separation between the source and the c.p.a. that is required to obtain maximum Doppler shift with a specific horizontal receiver offset.

Supplementing this plot is Table 3.1 that lists the variables associated with maximum Doppler conditions for various horizontal offsets. As stated for Equation (3.16), terms are normalized with respect to d, and are therefore dimensionless. For a particular

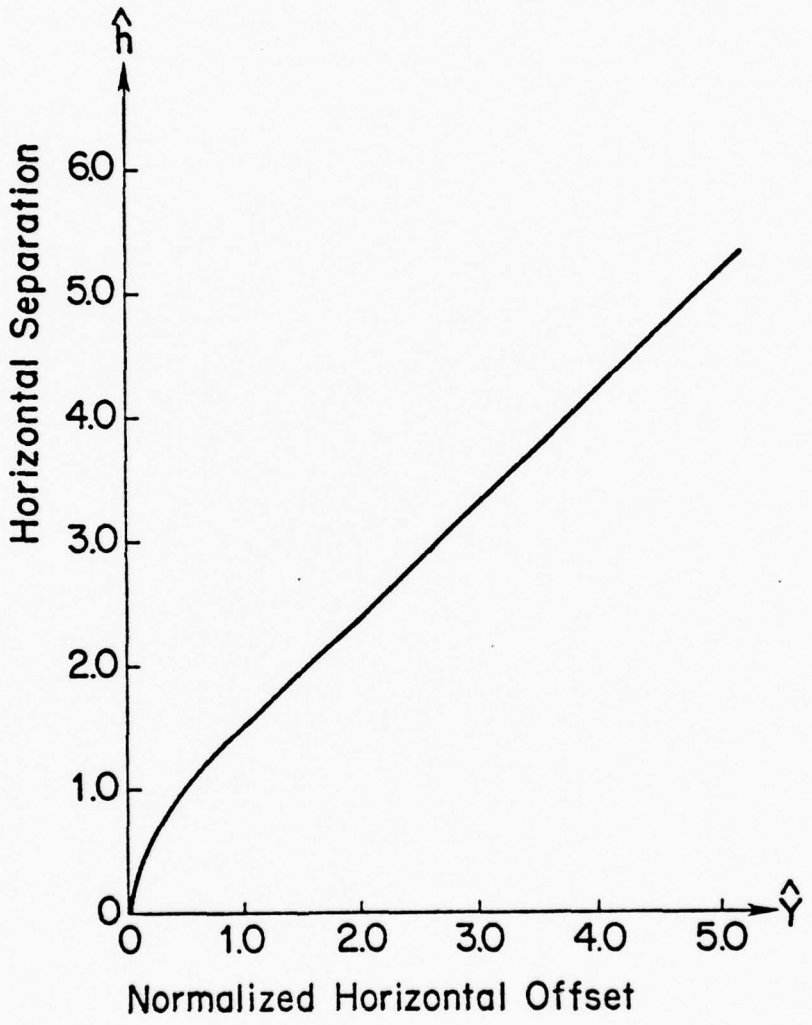

Figure 3.15 Relationship Between the Horizontal, Source-c.p.a. Separation and the Horizontal Offset for Maximum Doppler in a Refractive Medium.

TABLE 3.1

TABLE OF MAXIMUM DOPPLER PARAMETERS FOR
A HORIZONTALLY OFFSET RECEIVER IN A REFRACTIVE MEDIUM

$\hat{Y}$	$\hat{h}$	$\hat{H}$	θ	$\cos\theta$	ϕ	$\cos\phi$	max D
0.25	0.709	0.38	20.6°	0.94	19.6°	0.94	0.881
0.5	1.02	0.57	29.5°	0.87	25.7°	0.90	0.784
0.75	1.27	0.74	36.5°	0.80	30.3°	0.86	0.693
1.0	1.49	0.9	42.0°	0.74	33.9°	0.83	0.617
1.5	1.94	1.2	50.2°	0.64	37.6°	0.79	0.507
2.0	2.38	1.6	57.2°	0.54	40.0°	0.77	0.415
3.0	3.29	2.2	65.8°	0.41	42.4°	0.74	0.303
4.0	4.23	2.9	71.0°	0.33	43.4°	0.73	0.237
5.0	5.19	3.6	74.5°	0.27	43.9°	0.72	0.192

offset, the table lists the optimum horizontal source c.p.a. separation, along with the resulting $\hat{H}$. Also listed are the corresponding offset and emission angles which determine the magnitude of maximum Doppler presented to the receiver. This magnitude is normalized by v_s/c_s (maximum possible Doppler shift, see Section 3.1), so that in the table listing, it is given numerically as less than unity.

Figure 3.16 shows a comparison of maximum Doppler magnitudes (normalized by v_s/c_s) for two medium conditions. The solid curve represents the maximum Doppler magnitude as seen at a horizontally offset receiver in a refractive medium, plotted against the normalized value of receiver offset. It can be observed that the maximum obtainable Doppler magnitude diminishes with increased offset. This is because the offset and emission angles increase, even though the optimal relationship between $\hat{Y}$ and $\hat{h}$ is maintained.

The dashed curve is a plot of Doppler magnitude in the absence of ray refraction. Since this type of propagation will realize a maximum only for an offset angle of zero (no offset), the dashed curve does not represent maximum values, but rather those taken with the source at refracted ray optimum, source positions.

As a further illustration of the effect of a horizontal offset on Doppler, Figure 3.17 is provided. The curve in this figure represents refracted ray Doppler magnitudes plotted against $\hat{h}$, assuming the horizontal offset to be equal to d . The equation of this plot is derived from Equation (3.15) by normalizing with respect to d . This gives:

$$D = f\frac{v_s}{c_s} \frac{1}{(1 + H^2)^{1/2}} \times \frac{\hat{h}}{(\hat{Y}^2 + \hat{h}^2)^{1/2}} \quad . \qquad (3.17)$$

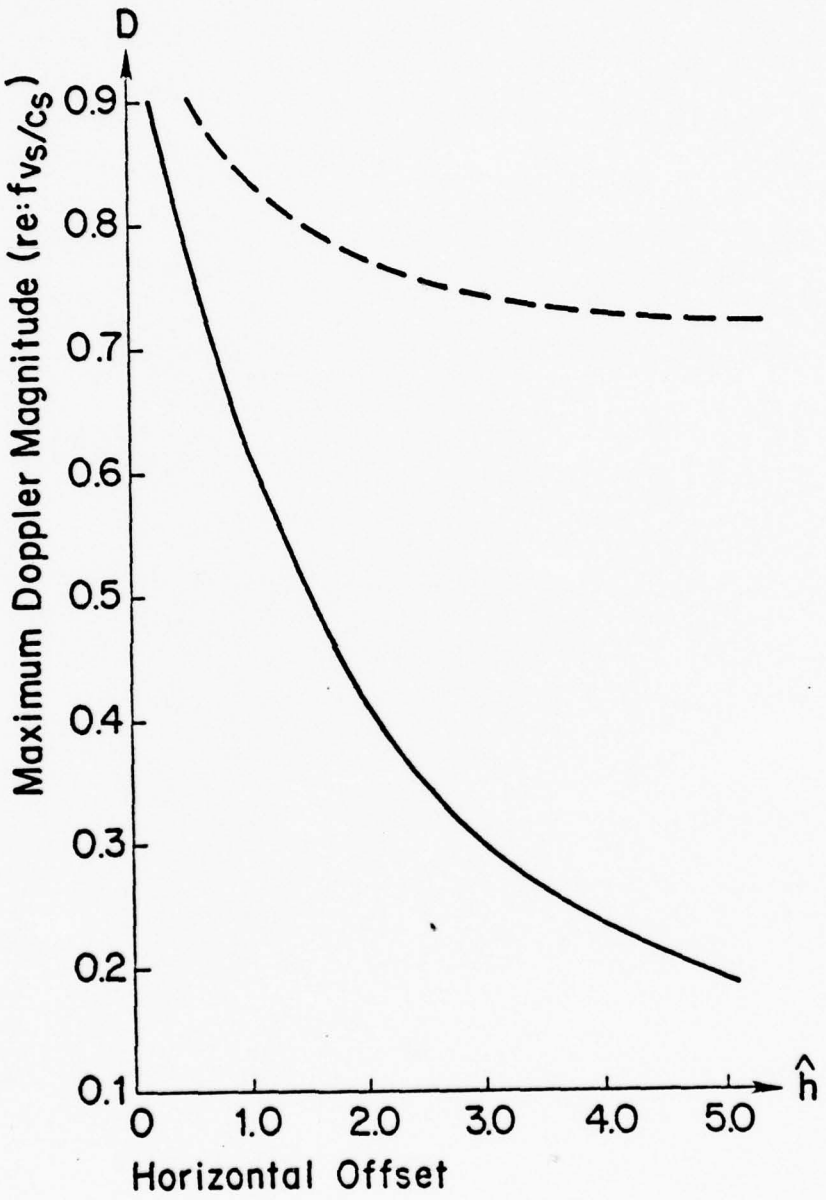

Figure 3.16 Comparison of Maximum Doppler Magnitudes Between Two Types of Ray Propagation when Viewed from a Horizontally Offset Receiver.

The solid curve represents refracted ray propagation, while the broken curve is for straight-line propagation.

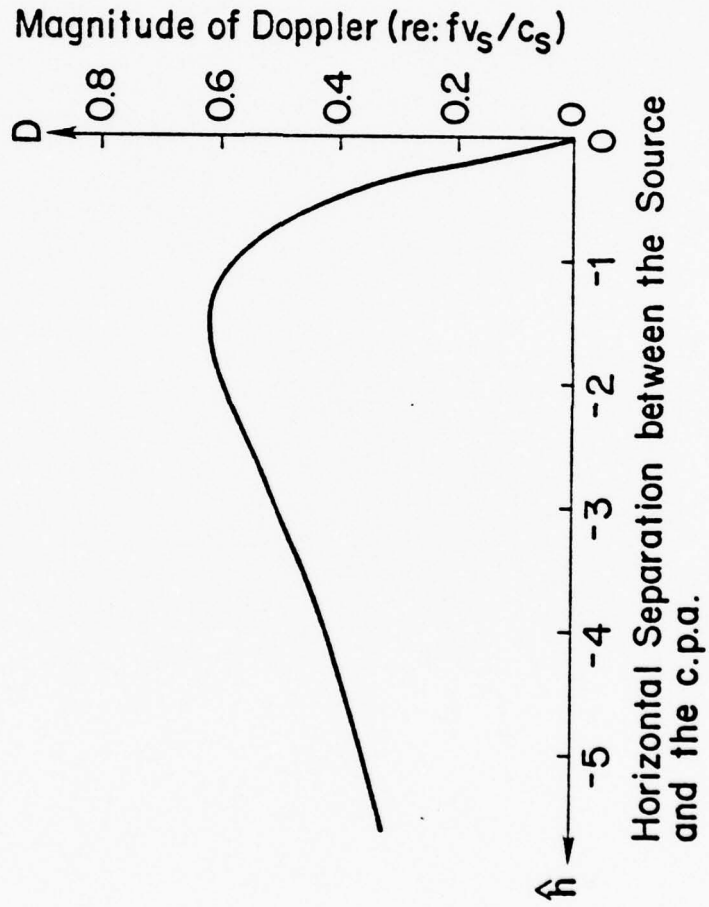

Figure 3.17 Refracted Ray Doppler Magnitude Seen by a Receiver with a Unity, Horizontal Receiver Offset.

When $\hat{Y}$ is zero, $\hat{H}$ equals $\hat{h}$, and this equation reduces to the form of Equation (3.3). This implies that the curve of Figure 3.17 is identical to that of Figure 3.3, excluding scaling.

The scaling of Figure 3.17 is done in proportion to the cosine of the offset angle--the larger the offset, the smaller the cosine of ϕ, resulting in a reduced magnitude of Doppler (with respect of v_s/c_s). This is consistent with Figure 3.16, where the magnitude of maximum Doppler reduced with increased offset.

3.4 Consideration of Multilayering

The general shapes of the Doppler magnitude plots obtained for the offset receiver in a single, linear-gradient layer will remain the same for a multilayered medium, except for the scaling change in the horizontal, source-receiver separation. This assumes that all of the gradients slope in the same direction.

Consider the three sound velocity profiles represented in Figure 3.18. One profile, shown as the solid line, consists of one gradient that characterizes a single layer. The other two, shown by a broken line in one case, and a double broken line in the other, have the same gradient as the single layer for their lower segment, but in their upper half, have gradients which are lesser and greater than that of the single (respectively). A ray, shown leaving the source at an angle of θ_1 from position S, intercepts the receiver. Position S' is where the source would have to be to produce a receiver-intercepting ray emission of the same angle (θ_1), should the steeper velocity profile (double broken line) define the medium. Likewise, position S" corresponds to the source location required by the broken line gradient.

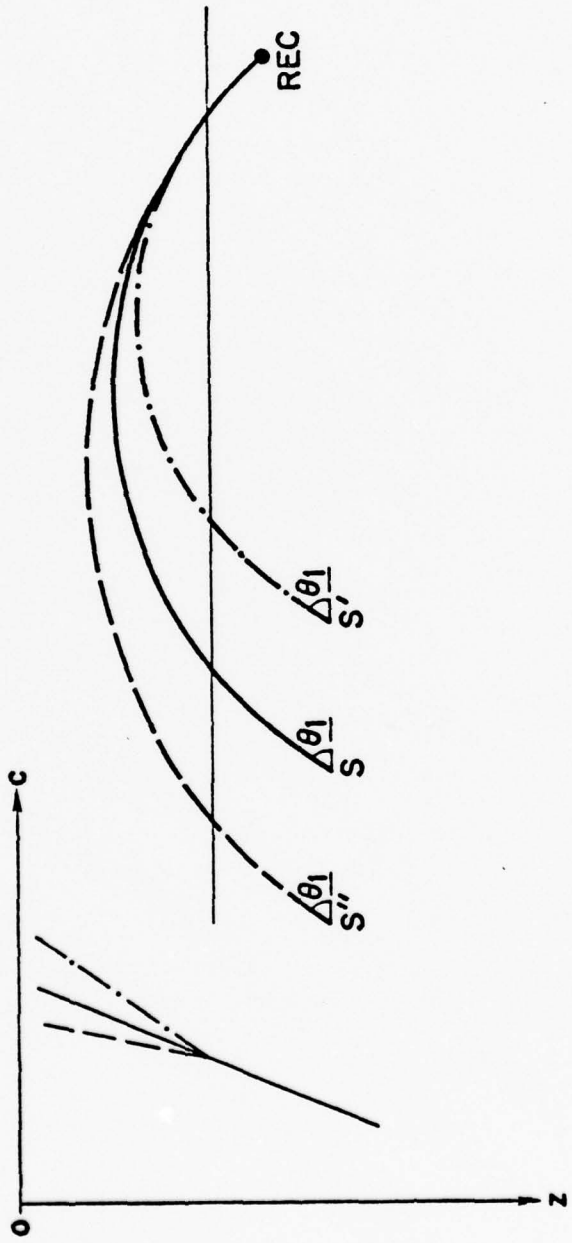

Figure 3.18 Velocity Profile-Dependent Source Positions for Rays of the Same Emission Angle.

This accounts for the scaling change mentioned above and applies when the source is far enough away from the receiver to allow receiver-intercepting propagation to penetrate a second layer.

CHAPTER IV

PRACTICAL CONSIDERATIONS

4.1 Preliminary Considerations

When straight-line ray paths are used to approximate propagation in a medium of velocity gradients, the Doppler shift expected at the receiver will be different from that which will actually be received from refracted rays. The magnitude of this error depends on the difference between the emission angles of a receiver-intercepting, refracted ray and its straight-line approximation. This difference angle will be larger for some geometric configurations than for others, depending on the maximum emission angle permitted in a particular layer (or series of layers). Therefore, representative limits of this error require investigation of the factors that place restrictions on refracted ray propagation in layers.

While our primary interest concerns the difference between refracted and straight-line rays, major emphasis will be placed on rays considered primary in a particular layer (or series of layers). To be classified as primary requires that the ray remain in its layer (or layer series) without boundary reflecting and without leaving the layer (series) previous to intercepting the receiver. Rays not meeting this criterion while intercepting the receiver are considered to be interfering with the reception of the primary signal. This interference has multiple consequences ranging from negative reinforcement of the desired signal, to frequency smearing of the received signal.

The negative reinforcement stems from surface reflections and path length differences between the primary and various interference signals. All of these are seen as phase different signals at the receiver.

Generally, interfering rays are emitted at larger angles than primary rays, resulting in Doppler shifts that are smaller for the interference rays than the primary. An exception to this occurs with very small angle SOFAR rays, which carry highly Doppler-shifted sound. The blending (i.e., non-distinction) of a multitude of these differently Doppler-shifted signals by the receiver results in a smearing of the conglomerate signal, since each signal is undergoing its own rate of change in Doppler (see Chapter III for these rates of change).

4.2 Limiting Ray of a Single Layer

The geometric parameters of a layer are significant when prescribing limits that ensure non-interfering propagation. Consider layer N in Figure 4.1, which contains a receiver, and where a reflected ray travels in the direction of increasing sound speed while being gradually bent in the direction of decreasing sound speed. The ray can enter the layer in one of two ways: by being emitted in the layer, or by entering the layer from some other layer.

Rays which propagate through layer N and are bent horizontally before intercepting the receiver have a limit imposed on their angle of entrance so as to meet the primary ray criterion. The maximum allowed angle, denoted as θ_{lim}, is associated with the limiting ray of the layer (illustrated in Figure 4.1). Should the layer interface (on which the limiting ray nearly impinges) be an abrupt change in gradient

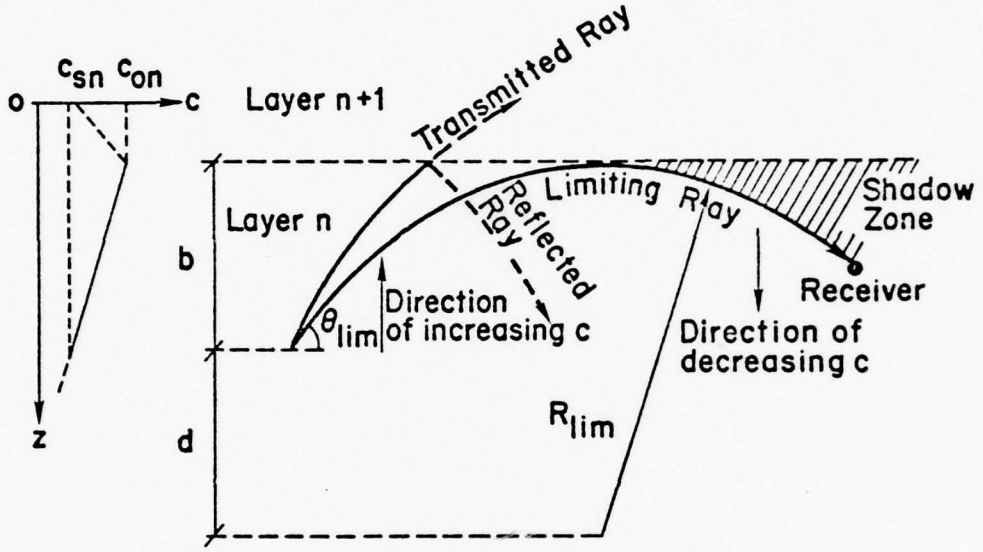

Figure 4.1 Limiting Ray in a Single Layer.

slope, or a medium boundary (such as the surface which acts like a gradient mirror), then the region beyond this limiting ray can be described as a shadow zone (as shown in the figure) since a receiver in that region is subject to receiving only interference rays. Any ray that enters (or is emitted in) layer N at an angle greater than θ_{lim} will either continue into the next higher layer (layer N + 1), or boundary reflect (if the layer borders with a boundary). The value of this maximum angle is determined by:

$$\theta_{lim} = \cos^{-1}\left(\frac{c}{gR}\right) \quad , \tag{4.1}$$

where c is determined at the point where the ray enters the layer. This equation can also be written as:

$$\cos\theta_{lim} = \frac{d}{R} \quad .$$

Since d can be expressed as the difference between the limiting radius of curvature, R_{lim}, and the thickness of the layer, b (see the end of Section III for a more precise definition of this quantity), this equation becomes:

$$\cos\theta_{lim} = 1 - \frac{b}{R_{lim}} \quad . \tag{4.2}$$

As a practical example, consider the three layers shown in Figure 4.2, each of which is defined by a typical negative gradient. These gradients are actually linear approximations to a sound velocity profile obtained from NADC Report NADC-AE-6647 (1966). It is desired that the angle of emission be determined for the limiting ray of each of these layers, assuming that each layer has a sound source at the

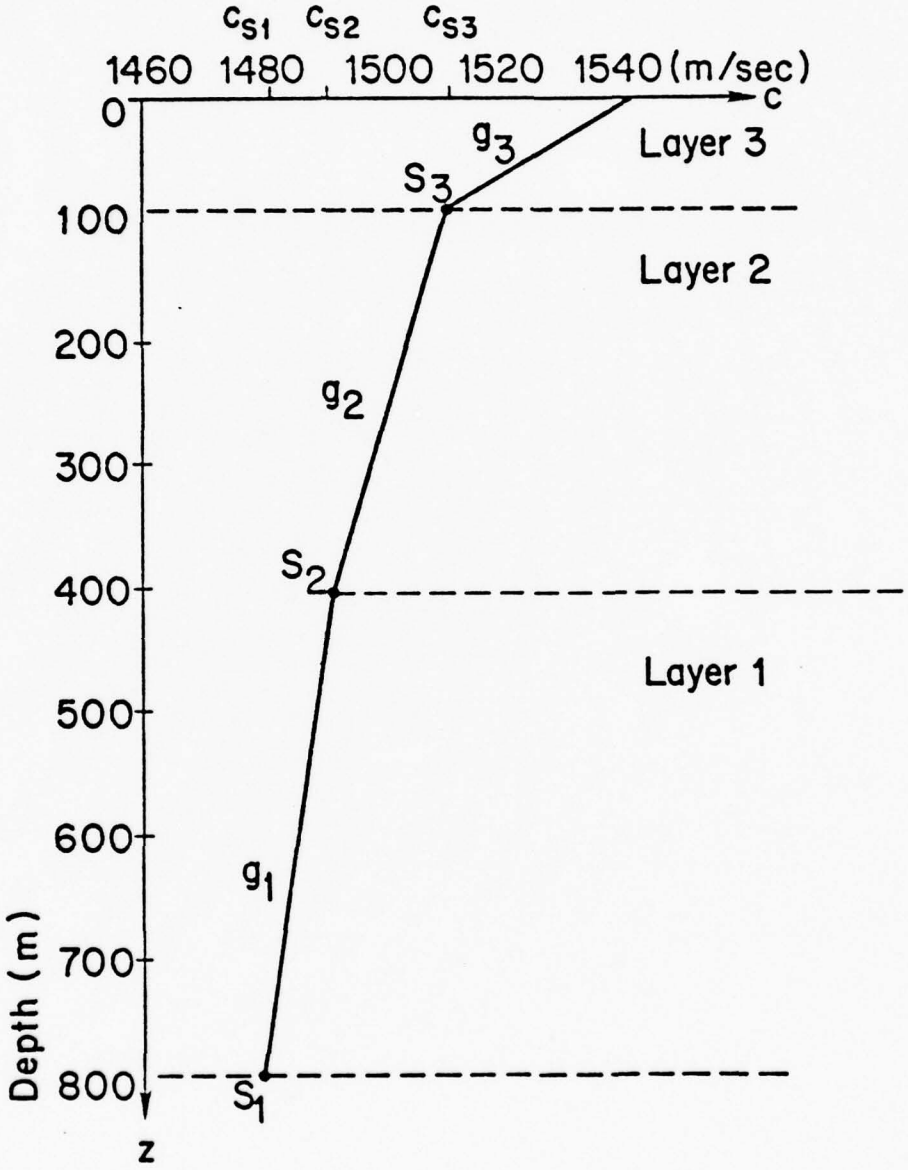

Figure 4.2 Typical Linear Approximations to a Negative Sound Velocity Gradient Which Produces a Multiple Layered Series.

bottom of the layer. The purpose of this is to provide some representative limits on primary ray propagation found in realistic layers. The following table supplies data pertinent to the three layers.

TABLE 4.1

CHARACTERISTICS OF THREE TYPICAL LAYERS

Layer	b (m)	Gradient (dc/dz) [(m/sec)/m]	c_s (m/sec)	R (km)
3	90	0.333	1512	4.5
2	315	7.95×10^{-2}	1487	18.7
1	385	1.82×10^{-2}	1480	81.3

The application of these data to Equation (4.2) produces the following values of limiting rays for the three layers:

$$\theta_{\text{lim } 3} = 11.5°$$
$$\theta_{\text{lim } 2} = 10.5°$$
$$\theta_{\text{lim } 1} = 5.6°$$

The relatively small limits on these angles (compared to those which might be expected when looking at the Doppler curves like Figure 3.3) can be attributed to the ray's large radius of curvature in a proportionately thin layer, resulting in a small b/R ratio. A large b/R indicates either a very deep layer or a very strong gradient (which produces a small radius of curvature). Figure 4.3 reveals the relationship between the b/R ratio and the limiting angle of emission,

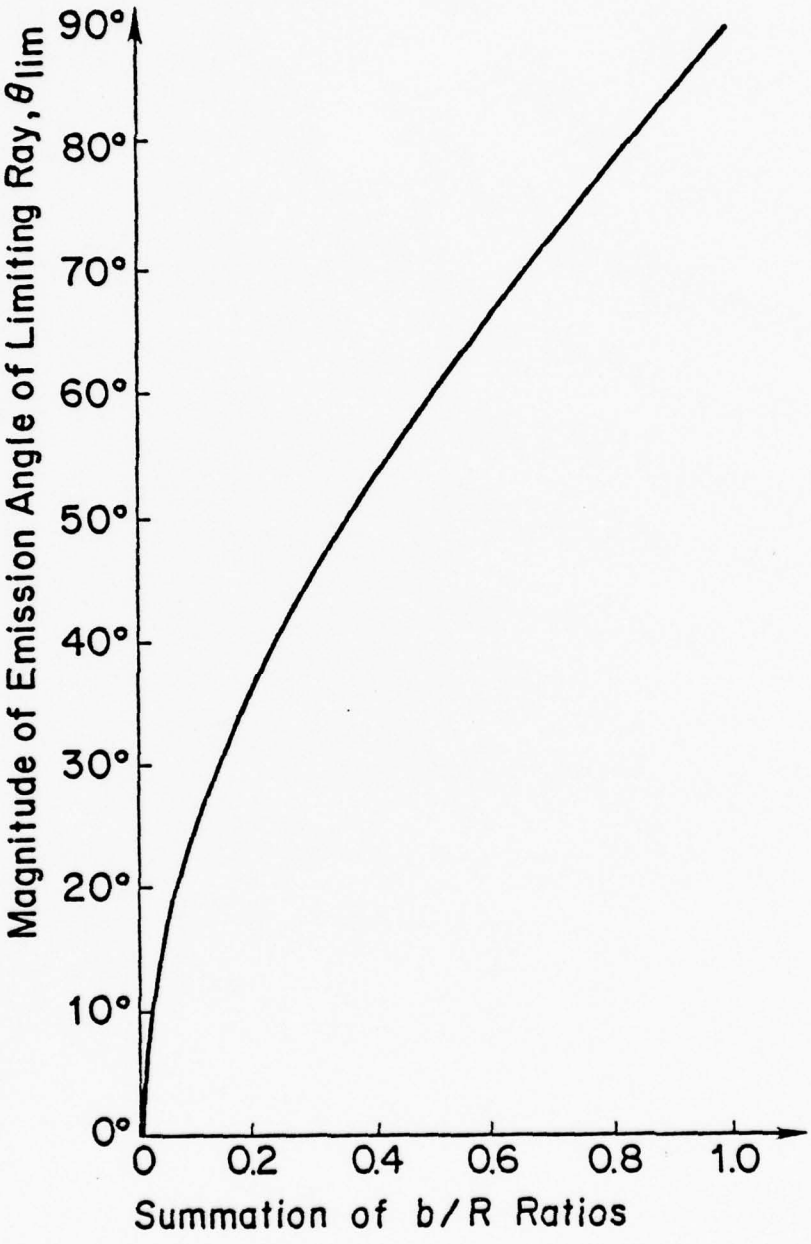

Figure 4.3 Relationship of b/R Ratio Summations to the Angle of Emission of Limiting Rays.

as prescribed by Equation (4.2). This ratio is actually a summation of ratios, one for each layer of ray travel. It will be described for multiple layers in Section 4.3.

Since the Doppler shift is proportional to the cosine of the emission angle, the smaller the b/R ratio, the larger the minimum Doppler seen at the receiver (the limiting ray is emitted at the largest angle of any primary ray, so it therefore carries the least Doppler-shifted sound).

The maximum horizontal source-receiver separation that can be reached by primary rays will occur for the limiting ray. It can be seen from Figure 3.2 that this maximum distance is related to the layer entrance angle by:

$$h_{max} = 2R \sin\theta_{lim} \quad .$$

For the three layers of Figure 4.2:

$$h_{max\ 3} = 1.8 \text{ km}$$

$$h_{max\ 2} = 6.8 \text{ km}$$

$$h_{max\ 3} = 15.8 \text{ km} \quad .$$

4.3 Multiple Layer Limiting Ray

The next consideration involves a ray emitted from a source in the layer below a surface-bordering layer--see Figure 4.4. For this ray to propagate through the layer of origin (layer 1) into the uppermost layer (layer 2) requires an emission angle that is greater than the limiting angle of the lower layer. To avoid surface reflecting, the ray must enter the uppermost layer at an angle that does not exceed $\theta_{lim\ 2}$, the limiting angle of that layer.

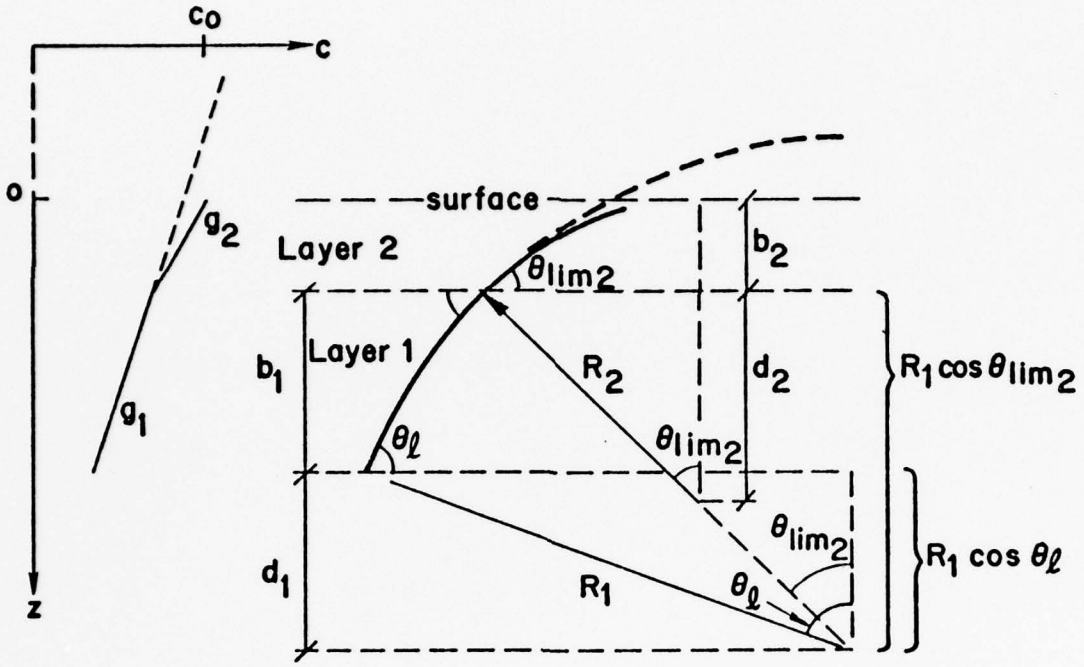

Figure 4.4 Refracted Ray Path of the Limiting Ray in a Multi-Layered Medium.

Since the ray originates in the lower layer at an angle of θ_ℓ, it is desirable to describe in terms of both layers' geometric parameters the maximum value of θ_ℓ that allows propagation into the upper layer while restricting the ray from surface reflecting. This is done by determining the thickness of the lower layer that extends above the point of the ray's origin to the layer. This thickness can be described as the difference between the two vertical projections of the radius of ray curvature taken at the deepest and the shallowest points that the ray traverses. This provides:

$$b_1 = R_1 \cos\theta_{\text{lim } 2} - R_1 \cos\theta_\ell$$

or

$$\frac{b_1}{R_1} = \cos\theta_{\text{lim } 2} - \cos\theta_\ell \quad . \tag{4.3}$$

Substituting from Equation (4.2):

$$\cos\theta_\ell = 1 - \frac{b_1}{R_1} - \frac{b_2}{R_2} \quad . \tag{4.4}$$

To ensure that this angle of emission will allow the ray to enter layer 2, θ_ℓ must be larger than $\theta_{\text{lim } 1}$, or:

$$\cos\theta_\ell < \cos\theta_{\text{lim } 1} \quad .$$

This is satisfied since the equality given in Equation (4.4) is smaller than that of Equation (4.2) (when applied to layer 2).

From the definition of the radius of curvature, Equation (4.4) becomes:

$$\cos\theta_\ell = 1 - \frac{b_1 g_1}{c_{o1}} - \frac{b_2 g_2}{c_{o2}} \quad , \tag{4.5}$$

where c_{o1} and c_{o2} are the speeds of sound where the ray becomes horizontal in the respective layers.

Since Snell's law required $c/\cos\theta$ to be constant at all points on a ray path, the speed of sound at which the ray would become horizontal in each layer must be the same. That is:

$$c_{o1} = c_{o2} \quad .$$

Hence, the speed of sound at which a particular ray would become horizontal is invariant to the gradient through which it travels. In light of this, Equation (4.5) becomes:

$$\cos\theta_{\ell} = 1 - \frac{b_1 g_1}{c_{o1}} - \frac{b_2 g_2}{c_{o1}} \quad . \tag{4.6}$$

This equation can be extended for the case where the ray propagates through N layers without boundary reflecting in the final layer. The angle of emission in the first of N layers is θ_{ℓ}, such that:

$$\cos\theta_{\ell} = 1 - \left(\frac{(b_1 g_1 + \ldots + b_N g_N)}{c_{o1}} \right) \quad . \tag{4.7}$$

The practical significance of this finding can be shown by applying it to the three typical layers previously discussed in Section 4.2. It is desired that the angle of ray emission from a source at the bottom of layer 1 be found such that the ray propagates through layers 1 and 2, subsequently becoming limiting in layer 3. This angle is found by substituting the appropriate data from Table 4.1 into the following form of Equation (4.7):

$$\theta_{\ell} = \cos^{-1} \left(1 - \frac{b_1 g_1 + b_2 g_2 + b_3 g_3}{c_{o1}} \right) \quad ,$$

where c_{o1} is the speed of sound where the ray is desired to be horizontal (i.e., near the surface, or top of layer 3). This provides an emission angle of:

$$\theta_{\ell} = 16.3° \quad .$$

As an alternative, the plot of Figure 4.3 can be used to determine the emission angle of the limiting ray in the final layer. This is accomplished by summing the b/R ratios of each layer through which the rays travel in going from the source to the final layer--refer to Equation (2.2) for determination of the radius of curvature in each layer.

Additional clarification of the term b is worthy of consideration at this point, since the definition of the term previously given did not cover all possible useage. For example, the b associated with rays that propagate through the entire thickness, or rays which enter the layer such that they are limiting in that layer, was prescribed in Section 4.2 and earlier in this section as equal to the thickness of the layer. However, this b, represented in Figure 4.5 as b_1, cannot adequately account for limiting rays emitted in the layer since the angle of emission is independent of b_1. The proper measure of b would span from the depth of ray origin to the depth of the highest sound velocity which the ray encounters in the layer. This is shown as b_2 in Figure 4.5. For sub-limiting rays emitted within the layer, b is measured from the depth of the source (or layer entrance) to the maximum depth of ray penetration in the layer. This is b_3 in the figure. One additional point must be stressed about the layer thickness extent (i.e., b) for rays emitted in the layer, since the measurements

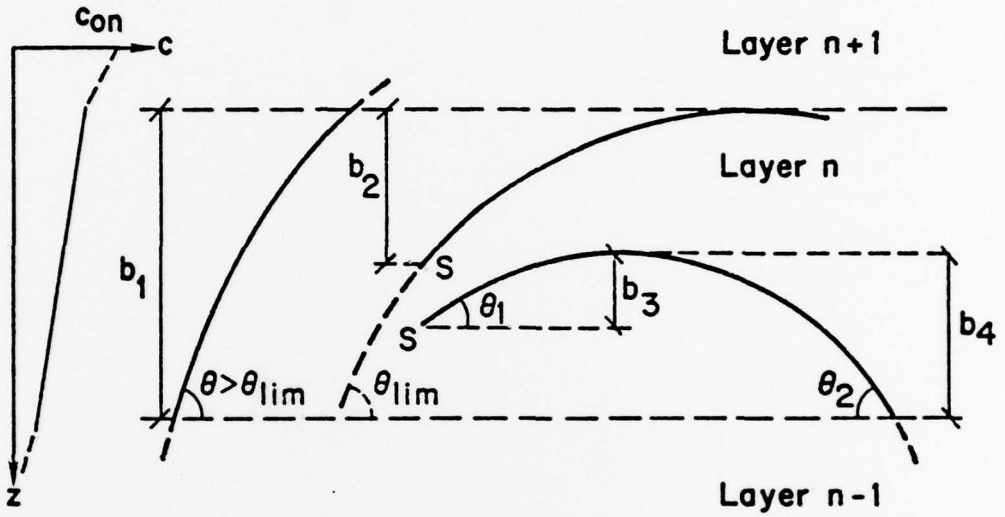

Figure 4.5 Possible Determinations of b .

of b listed above apply mostly to the angle of emission. The b used to determine the angle at which a ray (that has already been refracted beyond the horizontal position--i.e., a limiting or sub-limiting ray) leaves the layer (e.g., θ_2) is taken from the maximum depth of ray penetration to the depth where the ray exits the layer. This is exemplified by b_4 in Figure 4.5.

4.4 Doppler Error with Straight-Line Ray Approximations

4.4.1 Calculation of the Error. As previously stated, the Doppler shifts presented to the receiver by straight-line (non-refracted) rays or by refracted rays are different, depending on the difference between the projection of source velocity along each of them. The extent of the error depends on how close an approximation the straight-line rays are to the refracted rays. This error is given as a percentage of difference to the refracted-ray Doppler magnitude, such that:

$$\% \text{ Doppler Error} = \frac{\cos\theta_{\text{refracted}} - \cos\theta_{\text{approx}}}{\cos\theta_{\text{refracted}}} \times 100 \quad . \tag{4.8}$$

The absolute maximum error occurs whenever one of the rays carries maximally Doppler-shifted sound while the other bears true frequency (non-Doppler-shifted) sound.

Absolute maximum error is found at extreme separations between an in-line source and receiver, assuming that the straight-line approximations extend along the source path (see Section 3.1). As shown in Figure 3.1, the Doppler shift along straight-line rays is of constant, maximum magnitude up to the positive-to-negative transition.

Comparison of this to the curve of refracted ray Doppler in Figure 3.3 reveals that the larger the source-receiver separation, the larger the difference in Doppler shift between sound following the two types of ray paths. Theoretically, the refracted ray's Doppler magnitude will reach zero at an infinite source-receiver separation, while the straight-line Doppler maintains maximum magnitude. This provides absolute maximum Doppler error. However, zero Doppler shift requires a 90° angle of emission and (to reach the receiver) an infinite radius of curvature in an infinitely thick layer (to ensure non-reflecting propagation).

Layers of finite thickness impose a limit (equal to the limiting angle of the layer's critical ray) on the maximum emission angle of primary rays (see the two previous sections). This limit defines the relative maximum of Doppler presented to the receiver by straight-line approximations of refracted primary rays.

As a practical example, consider the uppermost layer of the three-layer series given in Figure 4.2. The limiting angle for primary ray propagation in this layer was previously found (Section 4.2) to be 11.5°. The difference in Doppler shift between this critical ray and its straight-line approximation is [from Equation (4.8)] slightly greater than 2%. For propagation through all three layers of Figure 4.2 (limiting angle of 16.3°), the error is 4.2%.

The magnitude of relative-maximum Doppler error corresponds to the b/R summation of the N layers of propagation. Substituting the relationship given in Equation (4.2) for the cosine of the refracted ray emission angle, and unity for the cosine of the straight-line ray emission angle, into Equation (4.8) results in:

$$\% \text{ Doppler Error} = \frac{\sum_{1}^{N} b_n/R_n}{1 - \sum_{1}^{N} b_n/R_n} \times 100 \quad .$$

For a series of layers with a b/R summation of 0.091 (corresponding to an emission angle of 24.62°), the Doppler error is 10%.

4.4.2 Boundary-Reflected Error. Boundary-reflected (interference) rays and their straight-line ray approximations are considered to be emitted from an image source. Since a boundary appears to be a mirror of sound velocity profile, a ray emitted from an image source undergoes two series of refraction, so that the ray appears to travel from image source to receiver similar to that of a one-cycle SOFAR ray. Just as for a SOFAR ray, the difference in angle between an image-emitted refracted ray and its approximation is small, resulting in a Doppler error that is much less than that of the critical ray.

4.4.3 Error with Vertical Offsets. In the event of a vertical receiver offset, straight-line approximations will leave the source at an angle (as opposed to following the source path at zero angle). This was illustrated in Figure 3.4a and described in Section 3.2. A magnitude of Doppler shift plot is also provided in Figure 3.5. The effect of a vertical offset on Doppler shift seen at the receiver has been discussed in detail in Section 3.2. It was shown that a vertical receiver offset causes a shifting of the point of maximum Doppler-shifted emission away from the c.p.a. An added effect is on Doppler error. The magnitude of Doppler shift seen along straight-line approximations is no longer constant (and maximum), but rather is dependent on an angle that

changes with source-c.p.a. separation. The Doppler error, therefore, depends not just on one changing Doppler shift, but two.

At large source-c.p.a. separations, refracted rays leave the source at large angles, contrary to their straight-line approximations, which leave at small angles. The resultant Doppler error in this region is similar to that of the in-line (non-offset) receiver, in that they both approach absolute maximum as the separation stretches to infinity.

As the source approaches the c.p.a., the emission angle of refracted rays which intercept the receiver decreases. The corresponding straight-line approximations, however, leave the source at angles of increasing magnitude. Eventually, a point is reached where a refracted ray and its approximation leave the source at angles of equal magnitude (the refracted ray leaves the source upward, the approximation downward). This point is observed as one of zero Doppler error (as observed at the receiver). The region between the zero Doppler error point and the c.p.a. produces refracted ray Doppler magnitudes that are larger than that of their straight-line approximations. The magnitude of Doppler error increases to a relative maximum as the source travels from the zero-error point to that at which refracted rays are horizontally emitted (point of maximum refracted ray Doppler). Once past this point, the source emits what will be refracted rays in a downward direction at an angle that quickly increases (approaches the angle of emission of straight-line rays) with diminishing source-receiver separation.

CHAPTER V

SUMMARY AND CONCLUSION

Doppler shift along refracted rays has been shown to be dependent on the projection of source velocity along the ray. For a horizontally traveling source, this is proportional to the emission angle of the ray. This angle is dependent on the geometry of the source-receiver situation which includes the gradients of traveled layers, horizontal source-receiver separation, and the horizontal and vertical receiver offsets from the source path.

The source parameters may be estimated from received Doppler-shifted sound when the emitted signal consists of a known frequency. As stated in Section 2.1, the Doppler shift can be found at any point along the ray path. It follows that the velocity of the source can be determined at any receiver point along the ray, given the elevation angle (angle of reception), the magnitude of Doppler shift, and the speed of sound at the reception point.

The addition of a vertical receiver offset complicates the geometric expression of refracted ray Doppler. As shown in the magnitude of Doppler plots for various normalized offsets (Figure 3.11), increasing the offset causes a shift in the point of maximum Doppler emission away from the c.p.a. (illustrated by the zero crossings of the derivative curves in Figure 3.12). This is further substantiated by the relationship expressed by Equation (3.16), which directly ties increasing horizontal separation to increasing horizontal offset. The interest in this point is due to its sustenance of zero rate of change in Doppler

shift, allowing accurate frequency analysis in the absence of signal smear.

The general effect on Doppler shift by a horizontal receiver offset with refracted ray propagation is to curtail the magnitude of Doppler. As for vertical offset, a shift away from the c.p.a. occurs for the point of maximum Doppler emission when the horizontal offset is increased. However, unlike vertical offset, increasing the horizontal offset reduces the magnitude of Doppler at all source-receiver separations.

In addition to showing the significance of ray refraction on Doppler shift, this paper has shown that the usual practice of assuming straight-line rays is sometimes inadequate. The Doppler error that results depends on the difference between the magnitudes of emission angles of refracted rays and their approximation. The most inappropriate time to use the approximation is for propagation occurring in thick layers with large gradients which permit refracted rays of large emission angles to propagate between a source and an in-line receiver. The larger the emission angle, the larger the Doppler error. For non-interfering sound propagation, the error is limited by the limiting ray of layers which allow its propagation. Straight-line ray approximations produce minimal Doppler error when the receiver is vertically offset in relatively shallow layers of small gradient (large radii of curvature).

This was primarily an analytical study which lends itself to computer application. The Doppler expressions and limits for non-interfering propagation, provided herein, can be incorporated into a

computer algorithm which would predict refracted ray Doppler shift at any number of receiver positions, once the necessary medium and source characteristics were inputted.

BIBLIOGRAPHY

Periodicals

Clark, J. G., Flanagan, R. P. and Weinberg, N. L., "Multipath Acoustic Propagation with a Moving Source in a Bounded Deep Ocean Channel," Journal of the Acoustical Society of America, (December 1976), 60, pp. 1274-1284.

Flanagan, R. P., Weinberg, N. L. and Clark, J. G., "Coherent Analysis of Ray Propagation with Moving Source and Fixed Receiver," Journal of the Acoustical Society of America, (December 1974), 56, pp. 1673-1680.

Gerlach, A. A., "Motion Induced Coherence Degradation in Passive Systems," Conference Record 1976 IEEE International Conference on Acoustics, Speech and Signal Processing, Philadelphia, PA, 1976, pp. 660-663.

Jacyna, G. M. and Jacobson, M. J., "Analysis of Source-Motion Effects on Transmission in the Deep Ocean," Journal of the Acoustical Society of America, (May 1977), 61, pp. 1153-1162.

Jacyna, G. M., Jacobson, M. J. and Clark, J. G., "General Treatment of Source Motion on the Total Acoustic Field with Application to an Isospeed Channel," Journal of the Acoustical Society of America, (October 1976), 60, pp. 815-824.

Rowlands, R. O. and Quinn, F. G., "The Spacing of Underwater Arrays for a Diversity Reception Acoustic Telemetering System," Proceedings of the 1967 National Telemetering Conference, San Francisco, CA, May 1967, pp. 266-271.

Books

Albers, V. M., Underwater Acoustics Handbook II, University Park, PA: The Pennsylvania State University Press, (1965).

Kinsler, L. E. and Frey, A. R., Fundamentals of Acoustics, New York, NY: John Wiley and Sons, Inc., (1962).

Officer, C. B., Introduction to the Theory of Sound Transmission, York, PA: The McGraw-Hill Book Company, Inc., (1958).

Velocity Profile Atlas of the North Atlantic, Volume I, U. S. Naval Air Development Center, Johnsville, PA: Report No. NADC-AE, 6647, December 1966.

DISTRIBUTION LIST

Commander (NSEA 09G32)
Naval Sea Systems Command
Department of the Navy
Washington, DC 20362 — Copies 1 and 2

Commander (NSEA 0342)
Naval Sea Systems Command
Department of the Navy
Washington, DC 20362 — Copies 3 and 4

Defense Documentation Center
5010 Duke Street
Cameron Station
Alexandria, VA 22314 — Copies 5 through 16